E-152

A Proposal to Test
A High Resolution, Single Bunch, Beam Profile Monitor at the SLAC Final Focus Test Beam

J. Norem, J. Dawson, W. Haberichter, W. Novak, L. Reed, X-F. Yang
Argonne National Laboratory, Argonne, IL, 60439, USA

J. Spencer
Stanford Linear Accelerator Center, Stanford, CA, 94309, USA

May 4, 1993

RECEIVED
MAY 4 1993

A High Resolution, Single Bunch Beam Profile Monitor Outline

Description
- Spatial Resolution
  - Simple Approximation
  - Fresnel Diffraction / Monte Carlo
- Counting Rate
  - Temporal Resolution from streak camera
- Other effects, Ion motion, self focusing, etc
- Critical Questions

Applications
- FFTB
  - Wake field effects etc
- Plasma Lens
  - Nonlinear profiles, Strength = f(z) for underdense lens
- Liquid Jet Target
- Collider Detector
  - Beamstrahlung, Backscattered Compton
  - Internal Radiation Problems / Beam line optics

Test Run At Argonne Advanced Photon Source
- Design / Status

Test at FFTB
- Profile Monitor Components
  - Foils
  - Collimators / movers
  - Detectors / Optics
  - Alignment / Ground Motion
  - Control System
  - Compatibility with other experiments,
    - QED, Laser Compton Monitor, Plasma Lens, Orsay
- Radiation effects
  - Beamline Shielding
    - Beam loss profile
    - Hadrons, m's, showers
    - Target thickness, additional shielding
  - Minimizing Backgrounds
    - Slot collimators
  - Radiation Hardness of components
- Requests for running time, space, etc

Appendicies:
- A) RSI Paper
- B) Hamamatsu streak camera data sheet
- C) Seismometer Data sheet
- D) 6/6/91 Note

Introduction

We would like to test a bremsstrahlung beam profile monitor which uses nonimaging optics to measure beam position and density profile, ($\rho(y)$ or $\rho(y,t)$), at the final focus of a beamline or collider.[1] The system could be extended to use laser backscattered photons for higher statistics and resolution, or to operate passively using beamstrahlung from e^+/e^- collisions in a HEP detector. The ultimate resolution of the system would be roughly 5 - 30 nm, and 200 fsec, depending on incident beam energy, the placement of components in the dump line, radiation spectrum and detector design. The technique could also be used to provide high precision, high frequency data for beam feedback systems.

Description

The system, Figure 1, consists of a bremsstrahlung radiator at the focus of the electron beam, a single sided collimator to produce a bremsstrahlung shadow, and a slit and detector system to measure the shape of the shadow edge.[2] The diagnostic slit can be either tilted or parallel with the primary collimator. The sharpness of the shadow is inversely proportional to the size of the spot at the bremsstrahlung source. Shielding, and perhaps sweeping magnets, are required to disperse and absorb electron and photon backgrounds. Finally, the bremsstrahlung photons will be detected using a Cherenkov counter preceeded by a pair converter.

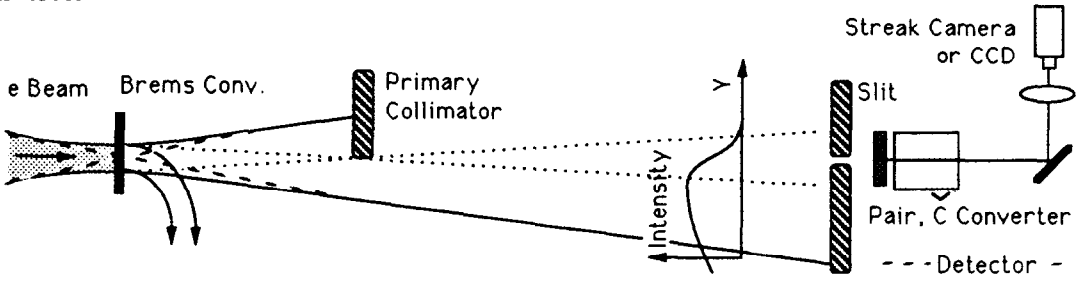

□ Figure 1. Bremsstrahlung radiator, single sided collimator, slit and detector.

Spatial Resolution

The ultimate resolution of this system is limited by Fresnel (circular wavefront) diffraction.[3] This limit can be approximated by using Fraunhofer (plane wave) diffraction and monochromatic light, (initially neglecting differences between measuring widths with first diffraction minimum, fitted σ, and FWHM). Consider a virtual slit at the primary single sided collimator location, where the virtual slit width is such that the sagitta is equal to λ, the photon wavelength. If the source to collimator distance is a, the collimator to detector distance is b, and $b >> a$, the expression for the sagitta $\lambda \sim s^2/2a$ gives the virtual slit width, $s = \sqrt{2a\lambda}$, (see Fig 2). The angular diffraction width is then λ/s and the limiting spatial resolution is roughly $(\lambda/s)a \sim \sqrt{\lambda a/2}$, nearly the geometric mean of the beamline dimensions, (1 - 10 m), and the photon wavelength, ($\sim 10^{-16}$ m at 10 GeV). Improving the resolution requires reducing a, by moving collimators close to the target, or reducing λ, by detecting the highest energy photons.

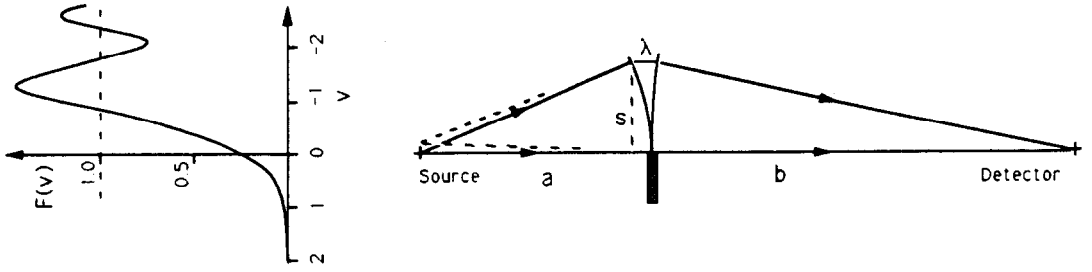

□ Figure 2. Fresnel optics. A point source produces a penumbra of finite width.

Accurate calculations of the resolution require: 1) Fresnel optics and 2) bremsstrahlung photon spectra modified by the detector acceptance. A precise calculation of the diffraction pattern is done for monochromatic light in most optics books. Integrating the intensity from all paths requires solving the Fresnel integrals, the solution of which generates the Cornu spiral. If the intensity of diffraction pattern on a screen is given by $F(y)$, the width of the pattern in terms of

$$y = v\sqrt{\frac{\lambda a(a+b)}{2b}}, \tag{1}$$

which gives the dimensions of diffraction patterns on a screen in terms of v, the dimensionless variable used to evaluate the Fresnel integrals[3]. For bremsstrahlung, the resolution of the system is then determined by incoherently adding diffraction images produced by the bremsstrahlung spectrum as seen by the detector.

The acceptance of the detector has been evaluated using EGS4 and a more specialized Monte Carlo program which generates a bremsstrahlung spectrum, computes pair production and subsequently evaluates multiple scattering[4]. The detected spectrum, which depends on electron energy, position and angle cuts, is shown in Fig. 3 for a minimum detected electron energy of 20 MeV and a maximum angle of 2°. Defining a resolution function as the derivative of this sum of diffraction images gives the curve shown in Fig 4. This curve, which is nongaussian, is the effective shape of a zero width beam at the bremsstrahlung radiator in the limit of a zero width slit at the detector. High energy photons contribute most of the resolution.

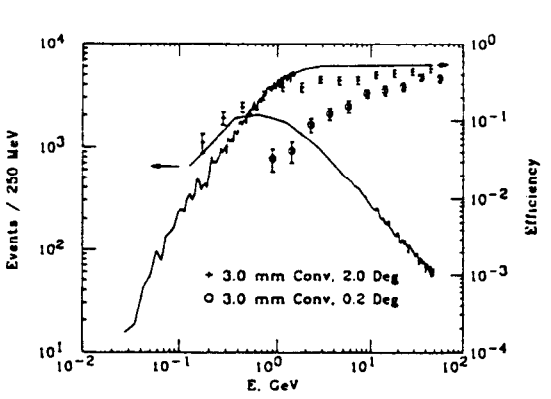

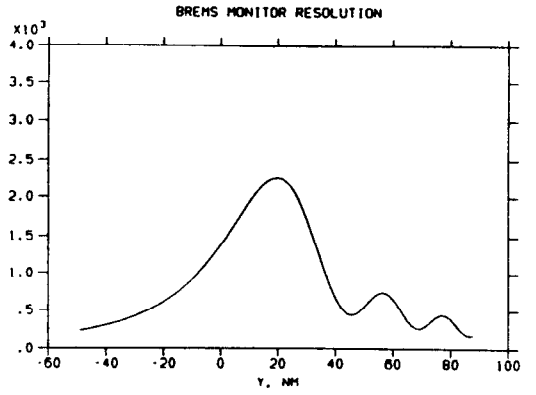

□ Figures 3 and 4. Monte Carlo simulations of the detection efficiency and photon spectrum for different pair acceptance angles, along with the resolution function for (E_e = 50 GeV, a=30, b=30m, θ_{pair} = 2°).

Detector

An option for the bremsstrahlung detector is shown in Fig 1, with a pair converter followed by Cherenkov radiator. Sweeping magnets may be required to reduce shower background. The total number of pair produced leptons $n_{e,pair} = n_{e,primary}(l/L_R)\eta(\phi/\sigma_{x',\gamma})$, where n_e is the number of electrons, l/L_R is the thickness of the bremsstrahlung radiator in radiation lengths ,L_R, η is the number of electrons detected for one equivalent full energy photon on the detector, which must be calculated by monte carlo and is roughly 1 - 10 depending on detector geometry, and $\phi/\sigma_{x'\gamma}$ is the acceptance of the detector slit divided by the divergence of the photon beam. In fact, the Monte Carlos calculate the flux of pair produced leptons of desired angle and energy for a given number of incident beam electrons, integrating over bremsstrahlung angle.

The number of Cherenkov photons produced would then be $n_\gamma \sim n_{e,pair}(L_{C,[cm]}/150)\sin^2\theta_C$, where L_C and θ_C are the length of the Cherenkov radiator and the Cherenkov angle,[5] which would yield $\sim$ 2000 photons in one Fresnel half width. It is assumed that Xe gas at 1 atm can be used as the Čerenkov radiator. With a refractive index n = 1.00071, the opening angle of radiation is 2.1°, and the minimum detectable electron energy is $\sim$ 12 MeV. Assuming the pair converter is 3.6 mm of tungsten and the Č radiator is 2 cm thick, the combined width due to pair production / shower dimensions and Čerenkov optics is $\sim 100\mu$.

Time Resolution

The number cerenkov photons should be sufficient to produce streak camera images with very good resolution using a Hamamatsu FESCA-500 streak camera, that has a time resolution of $\sigma_t \sim 200$, (FWHM = 400 - 450 fsec). This resolution requires very narrow slit opening, ΔS = 10 μm, and about 10 photons/channel to give a detectible signal. It seems desirable to consider solid Cerenkov radiators with large θ_C to give the maximum number of photons when streak camera measurements are desired. See Appendix B.

Ion Motion, Beam Focusing and Other Effects

Ionization of the bremsstrahlung radiator, motion of the target ions, multiple scattering, depth of focus, beam focusing by the plasma created in the radiator, and synchrotron radiation by the primary electrons, should be detectable, and correctable effects (Appendix A and D). It seems most useful to evaluate these effects relative to the beam divergence at the focus, 0.6 mr[4]. Multiple scattering is, $\theta_{MS} = 0.015\sqrt{l/L_R}/p_{[GeV]} = 0.1$ mr for FFTB parameters. Focusing due to plasma effects produces deflections of $\theta_f \sim 2B_\phi\sigma_z/B\rho \sim 0.2$ mr, with $B_\phi \sim \mu_0 I/4\sqrt{2\pi}\sigma_x \sim 50$ T. Synchrotron radiation in this field will have a critical energy of about 100 MeV, ($\Upsilon = u_c/E_e \sim 0.002$), but the number of photons produced and the total energy lost by this mechanism will be much smaller than bremsstrahlung. The opening angle for bremsstrahlung photons is $\theta_b \sim m_e/E_e \sim 0.01$ mr, which is negligible.[6] The depth of focus requires that the thickness of the bremsstrahlung radiator be $t \sim \beta_y^* = 0.1$ mm $\sim 0.03\ L_R$. The density of the bremsstrahlung radiator will change during the passage of the beam, since ions would move in the beam electric field. The ions are multiply ionized by electron collisions. Preliminary estimates of the density fluctuation give $\Delta n/n \sim 0.1$, which indicates the effect should probably be evaluated more carefully.

Shielding

The operation of this system, in particular the insertion of the bremsstrahlung radiator at the focus, will produce two shielding problems. First, the detectors must be shielded from electromagnetic showers to produce the maximum signal to noise ratio, and second, the beamline must be operated so that radiation levels outside the FFTB shielding enclosure due to the bremsstrahlung radiator are within DOE and SLAC radiation safety guidelines. [7] [8]

Critical Questions

A number of issues are raised in evaluating this technique for linear colliders. Since the ultimate resolution of the system is primarily determined by two parameters, a, the distance between the bremsstrahlung radiator and the primary collimator, and the detected spectrum of bremsstrahlung, it would be desirable to know experimental limits on these. The limits on a are primarily determined by radiation, heating and shielding effects, and the limits on the detected bremsstrahlung spectrum are determined primarily by backgrounds and shielding. Evaluation of the technique with backscattered Compton photons would also be useful.

Applications / Extensions

FFTB

Although two dimensional, f(x,y), profiles have been produced near the exit of the linac using synchrotron radiation [10], it would be highly desirable to make measurements of the beam profile, $f(y,t)$, at the focus, in order to study single or multibunch beam instabilities driven by wake fields and possible nonlinearities due to beam optics. The high resolution of this technique should permit study of a variety of other effects, such as the Oide limit, where beam size as a function of emittance, $\sigma \propto \epsilon^{5/7}$ [?], beam jitter or special tuning used for crab crossing. Weaker beams could be observed with thicker targets, without degrading

signal/noise, since both signal and noise should be a function of the beam on target.

Plasma Lens Studies

This method of beam profile monitoring was initially devised to examine plasma lens focusing, where the capability of essentially imaging two dimensional beam profiles in a highly perturbed environment was desired. Plasma focusing is inherently nonlinear, due to inhomogeneities in the transverse and longitudinal charge density, plasma response time, $1/\omega_p$, and uneven plasma ionization. In addition, since plasma focusing is self focusing, beam jitter cannot be corrected, thus accurate profiles require single bunch measurements where jitter and focus effects can be independently isolated. The proposed technique should accomplish this.

Argonne experiments at 20 MeV show significant nonlinearities in both r and t [11]. At SLAC energies, higher plasma densities will reduce the response time, so that only underdense plasmas will show time dependent focusing.

Linear Collider Detector

The proposed technique of beam profile monitoring can be used either for single beams, or for continuous, passive, beam position and profile monitoring in the HEP detector of a linear collider. Single beam profiles would require the insertion of a thin target into the IP region of the HEP detector, (Fig 5), or a laser beam target for laser backscattering. Continuous monitoring could be done with beamstrahlung from e^+/e^- collisions. With beamstrahlung, resolution is limited by photon energy when the average beamstrahlung photon is a small fraction, Υ, of the incident electron energy. (Values of Υ depend on design, but average approximately 0.1, producing a photon spectrum peaked at lower energies than a bremsstrahlung target.[12] Even lower values would be common during tune up.) Backscattered photons, on the other hand can have very high energy and statistics, giving very good resolution, but require good laser timing, typically ≤ 0.3 ps.

For single beams, a bremsstrahlung radiator can be quite small and light, and, since the z position needs to be determined only to some fraction of $\beta^* \sim 0.1$ mm, the required positioning tolerances are not challenging. While the design of the target holder, collimators and detector would pose significant problems, the most significant interaction with the detector design may be the spray from the bremsstrahlung target[13].

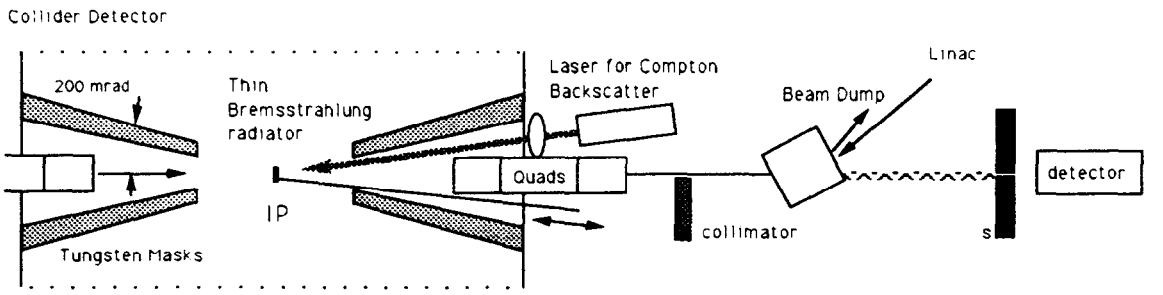

□ Figure 5. Schematic of operation with a collider detector.

While a high Z bremsstrahlung target at the IP would be a copious source of shower secondaries and radiation damage, the magnitude and composition of these showers should be somewhat similar to showers produced by beamstrahlung from e^+/e^- collisions. Recent

designs assume beamstrahlung energy loss δ of around 0.05, about the same from a thick bremsstrahlung target. [9] [14]

Designs for HEP detectors include tungsten masks to prevent low energy beamstrahlung secondaries emitted at angles of less than 200 mrad from entering the detector and these masks should also be useful for bremsstrahlung. Calculations using EGS4 have been done to examine the secondaries produced by such a target. The results, Fig 6, show the secondary electrons and positrons as a function of perpendicular momentum and angle, compared to beamstrahlung [15]. While the number of very low energy secondaries produced at large angles should be $< 10^{-6}\ n_{inc}$ which should be tolerable. Comparatively thin shielding, a pipe 0.5 cm thick, reduces the flux by another factor of about 10, i.e. that nothing is seen at angles greater than 70 mrad.

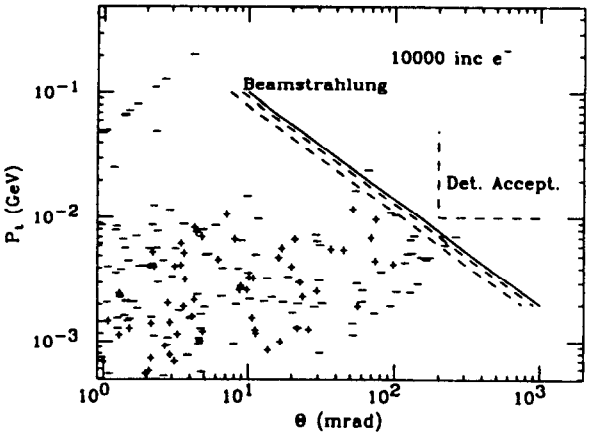

□ Figure 6. Production of secondaries in a foil.

The resolution of a bremsstrahlung system in a linear collider environment would depend on the placement of the primary collimator (and its shielding) in the dump line and the spectrum of detected photons. Scaling the resolution by $\sqrt{\lambda a}$ and assuming the fraction E_{det}/E_{max} is the same as for the FFTB experiment and collimators would utilize the space behind the quads 5 - 10 m from the IP, gives a resolution of on the order of 10 nm. Backscattered photons, on the other hand, efficiently produce very high energy photons and could produce resolutions on the order of 5 nm. An advantage of laser targets would be that optical pulses could be timed to examine specific bunches within a linac pulse to look for instabilities, jitter or other effects.

Liquid Metal Target

While the time resolution of the detectors and electronics is very good, solid bremsstrahlung targets would be vaporized by the beam, and would not be able to detect bunches other than the first of a series. A possible solution of this problem is the liquid metal jet being developed at SLAC by F. Villa. [16] If the target was moving at a speed of 100 m/s it would move 100 nm in 1 ns, approximately the beam size and approximate bunch spacing in collider designs. Comparatively large jets ($\sim$ 100 μ)could be used, which should be quite reliable.

Test Run at the Argonne APS Linac

The Argonne Advanced Photon Source (APS) is scheduled to be completed in 1995, and the electron/positron linac injector should be running in the summer of 1993. Parasitic bremsstrahlung from the positron production target can provide a useful test of the proposed system, because the electron beam energy is high enough to be detected (200 MeV), and high enough to produce a realistic shower background, and there should be sufficient space downstream of the positron linac to mount collimators, slits and detectors. The overall plan is shown in Fig 7.

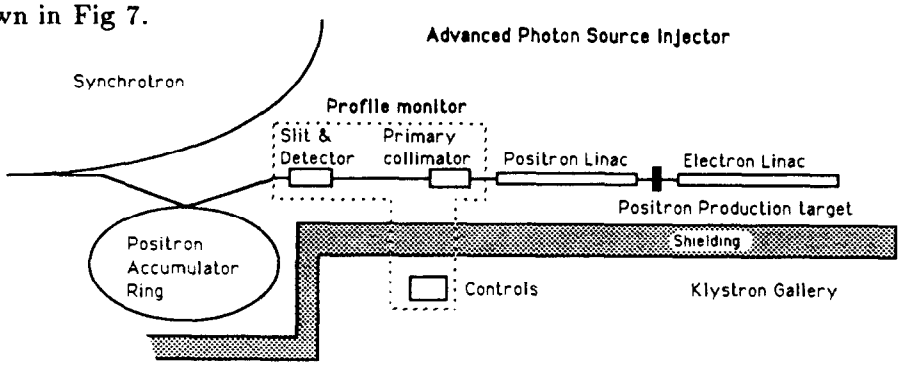

□ Figure 7, The test run at the Argonne APS Linac

Collimators are operated using encodermotors which should provide repeatable positioning to 0.1 μm. The collimator mounts, Cerenkov cell and optics are mounted on an optical breadboard. An image intensifier is used to increase the signal which is read out by a CCD linear image sensor. The whole system is controlled, using LabWindows, by a 486 computer with a camac interface.

Test at the SLAC FFTB

Profile monitor components

Present plans for installation in the FFTB are shown in Fig 8. The primary collimator would be located about 6 m downstream of the bending magnets and 27 m from the IP. Two components would be mounted here: the primary precision collimator: a 3" diameter tungsten mirror, ground and optically polished flat, and a slot collimator system, consisting of two tungsten or tantalum blocks ground flat and spaced apart by 0.00025" - 0.001" with shims. The guard collimator would serve two purposes: minimizing beam heating and deflection of the primary collimator, and providing a "black" background against which the beam on target can be seen.

The detector and slit are presently planned to be located on the muon shielding downstream of the dump. Another guard collimator would be located near the upstream wall of the beam dump enclosure. Again two heavy blocks would be used separated by thin shims. This guard collimator would be used to prohibit shower secondaries from escaping from the dump enclosure while permitting a good signal/noise for photons from the bremsstrahlung target.

The detector itself, which would consist of the pair converter, Cerenkov radiator, optics and CCD camera (or streak camera) would be located on the muon shielding, in a minimal restricted enclosure with a tungsten backstop. Locating the detector, slit and camera in a low radiation environment is useful to minimize backgrounds and irradiation of components as well as improving signal/noise ratio.

Vacuum requirements should be minimal. All slits and collimators could be in air, between sections of the E-144 vacuum pipe.

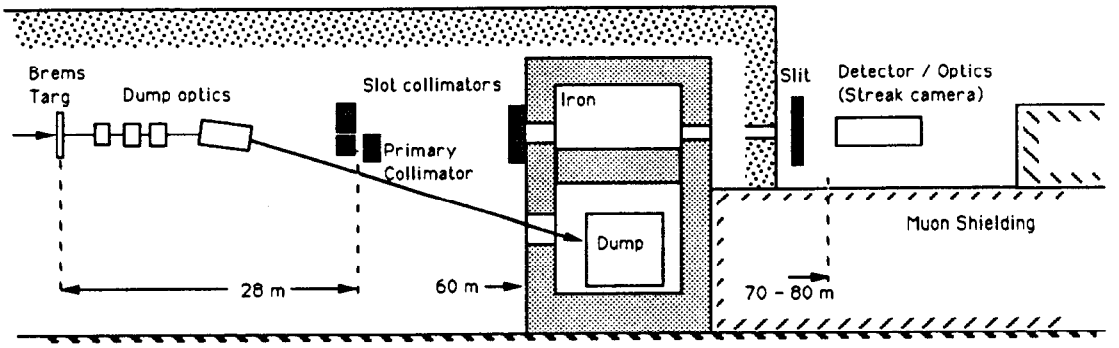

□ Figure 8, General location of components in the FFTB area.

Bremsstrahlung radiator: It is assumed that high Z materials will be used for the foil and these would be locally destroyed on every pulse. Energy deposited in the foil due to dE/dx losses would be on the order of 0.6 mJ/pulse. This energy would be sufficient to vaporize a hole 10 μ in radius in a tungsten foil. The foil will sit on a gearhead so it can be rotated as needed to a new spot after each bunch. Possible materials would include Ta, W, Pt, U, and Au, all of which are dense enough to permit the foil to be thinner than β^*. These foils are sold in many thicknesses and sizes by Goodfellow Corporation.[17], . Tungsten and tantalum have the highest heat of vaporization, which seems to be the best measure of their stability, but platinum, uranium or gold foils should also be useful. The target insertion mechanism proposed by P. Kwok of UCLA, shown in Figure 9 below, will be interlocked to permit only foils to touch the beam.

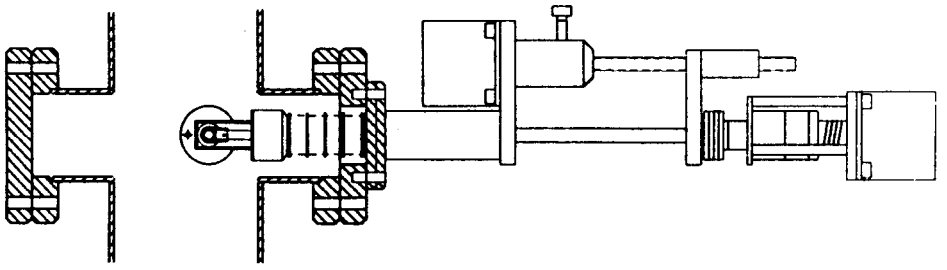

□ Figure 9. The Bremsstrahlung target insertion mechanism.

Collimators / Movers: The collimators have to be flat and thick enough to stop the beam. Tungsten mirrors can be produced which are 3" in diameter and optically flat, $\lambda/20 \Leftrightarrow (\sigma_z \sim$ 10 nm), for reasonable prices (and higher precision for higher prices).[18] (With a radiation length of about 0.31 cm, direct photons would be attenuated by $exp(-7.5/0.31) \sim 10^{-11}$ if they penetrate the collimator.

Encodermotors or stepping motors are sold which have setting errors of about $\sigma \sim 30$ nm, which should be sufficient. Finer motions can be achieved with peizomovers. It is assumed that the single sided collimator would not need to be cooled, although it might be desirable to mount them on materials with low coefficient of expansion such as invar or zerodur. Protective collimators should be cooled, recording position and temperature.

Detector / Optics: If located behind the beam dump on the muon shield, the slit and detector could be compactly mounted in a small enclosure. While the slit must be precisely located, the pair converter / cerenkov radiator assembly, along with the optics and camera can be located with some flexibility. Mirror optics have been used to minimize chromatic effects and UV absorption.

The camera, shown in Figure 10, uses a Hamamatsu V4183U two stage, gated image intensifier which has single photon sensitivity, mechanically in contact with a Hamamatsu S3902 MOS linear image sensor.[19] Fiber optic exit and entrance windows permit high resolution. Measurements of single photons have shown that the resolution is very good, $\sigma \sim 25$ μ, depending somewhat on pulse height. The radiation sensitivity of this system has been tested and it should operate well in a 100 mR/hr envionment. The manufacturer claims that the components should not be particularly sensitive to radiation damage.

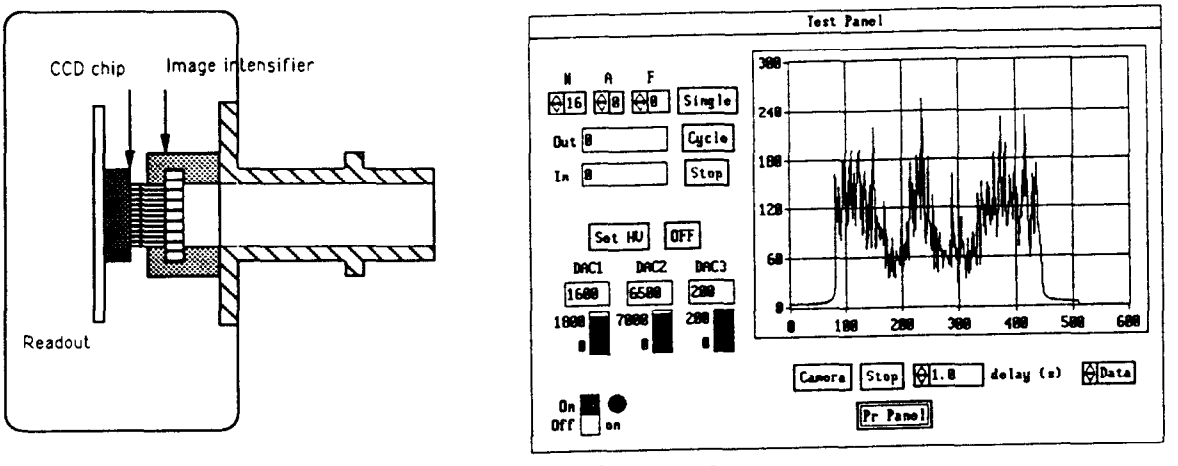

□ Figure 10. The camera with test graphic interface.

A streak camera would be highly desirable for intrabunch measurements, and could be easily incorporated into the optics. The Hamamatsu FESCA-500 is the only system which seems to provide the resolution necessary to resolve structure within the SLC bunch length (see Appendix B). With a clean signal it might be possible to operate the streak camera in a "slitless" mode, since the cerenkov light would be produced along a line 100 μ wide defined by the upstream bremsstrahlung slits and bremsstrahlung. A 10/1 reduction of image size would be desirable to efficiently image the 100 μ electron beam to a 10 μ size on the streak tube.

Alignment / Ground Motion: It is assumed that the system can be roughly aligned using transits and levels to about 100 μ. At that point it should be possible to use bremsstrahlung signals to align the system using the remote movers.

Ground motion would cause problems at two levels.[20] Slow drifts would change alignment

by 100~300 nm over periods of 10 seconds, and higher frequency oscillations would cause oscillations of about 10 nm at the beam pulse frequency. We plan to have a seismic correction system which can compensate these motions and have ordered a seismometer which should have sufficient precision to detect and correct them, either on line with piezomovers, or off line by correcting the data. (See Appendix C)

Control System: The control system is shown in Fig 11. It uses LabWindows to control 486 clone / camac hardware. The system has been operational in a minimal form since October 92 and has been evolving and improving. The seismic control functions have not been implemented because the seismometer has not been delivered, however all other functions work at some level.

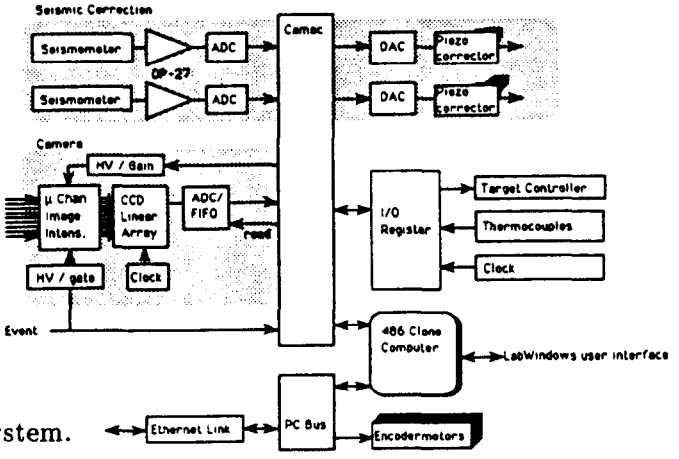

□Figure 11, The control system.

Compatibility with other Experiments: The aim of any beam diagnostic development should be to produce a technique that would be generally useful. The intention of this proposal will be to leave an operating system at the FFTB for use with other experiments. This device should complement and extend all the experiments planned for the FFTB in some way.

Although the IP and downstream hardware make this technique physically incompatible with the Orsay and Compton backscattered photon beam size monitors, the three should produce complementary data of roughly similar precision. [21] [22] By systematically comparing the results it should be possible to produce more reliable data on beam size, profile and jitter than could be obtained from a single method.

Interactions with the plasma lens experiment should be more significant, since the proposed diagnostic should have the spatial and time resolution sufficient to examine nonlinear plasma and beam effects directly and to clearly separate jitter from other effects.

It would be highly desirable to attempt beam profiles using backscattered Compton photons from the E-144 interaction region, to evaluate the technique for linear colliders. Laser beam profiles would be produced, since the laser spot would be smaller than the electron beam. The slot collimators constructed to reduce backgrounds in this experiment should perform the same function to help isolate high energy photons and reduce backgrounds in E-144.

Radiation Effects

There are three radiation problems associated with this experiment: personnel shielding of the beamline when the bremsstrahlung radiator is inserted, optimizing signal/noise seen by

□ Figure 12, Tracking the degraded electron beam using TURTLE.

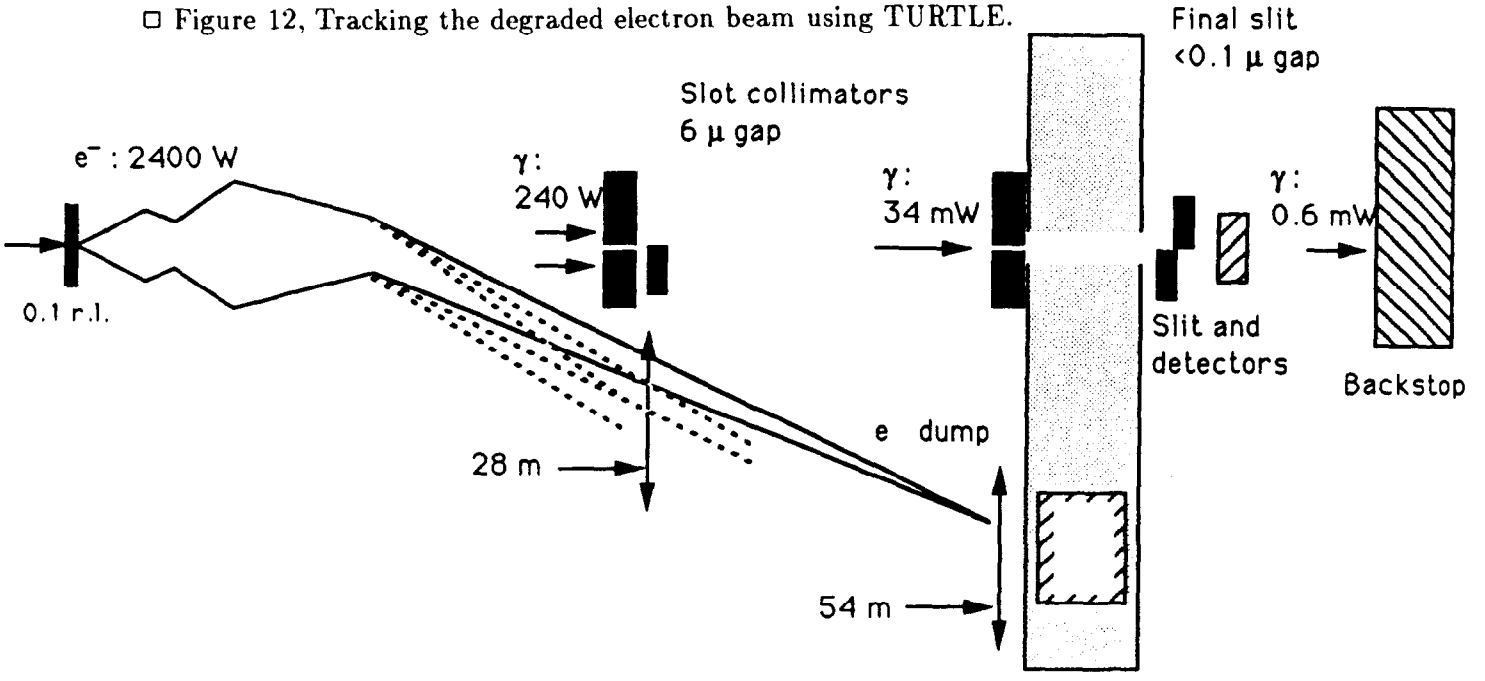

Profiles of Degraded Beam

28 m

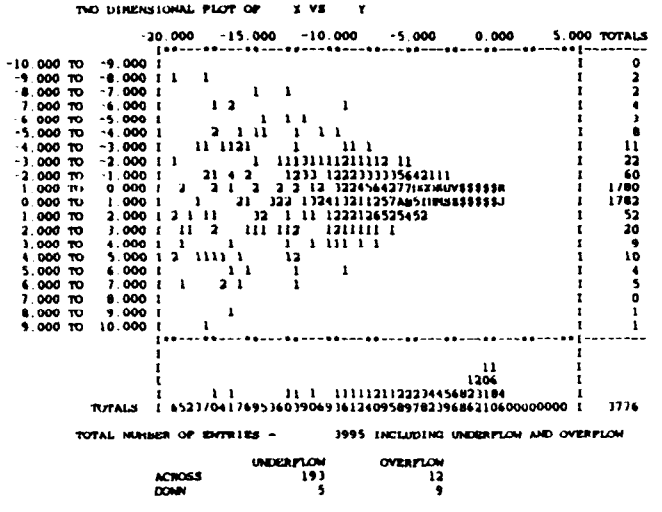

54 m

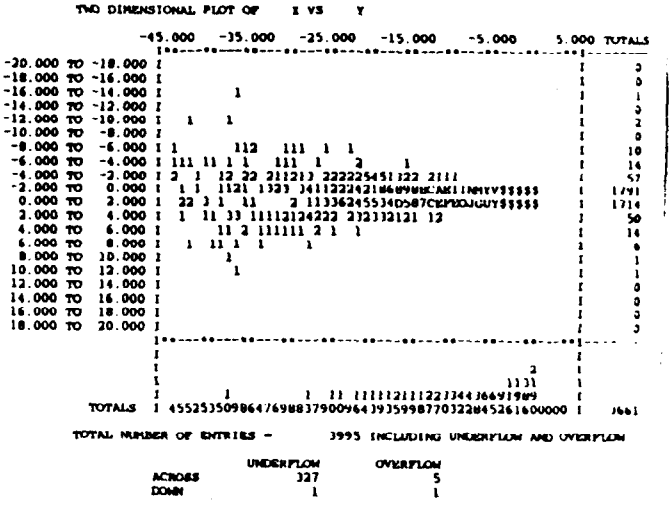

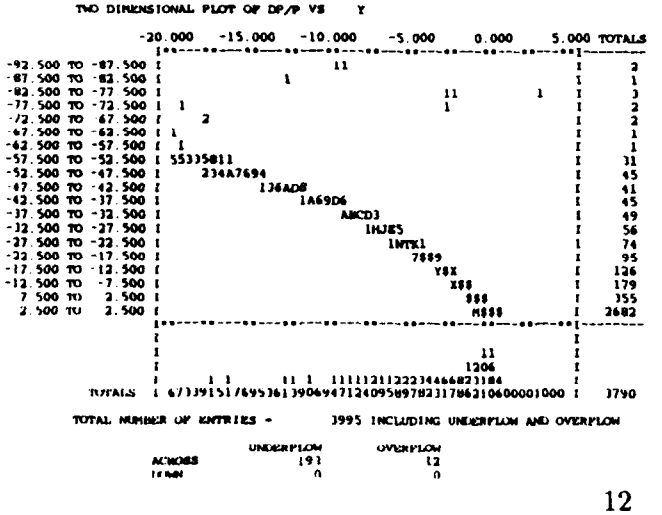

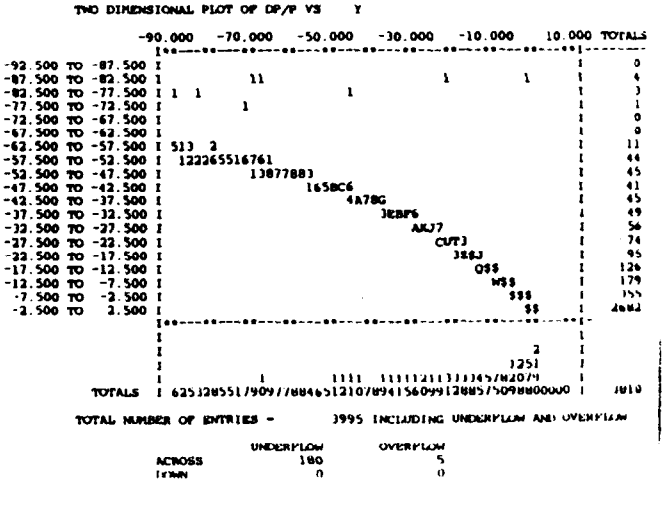

the detector, and preventing failures caused by radiation damage. It is hoped that all these problems can be solved by additional shielding, and possibly insertion of the target at a lower rate.

Beamline Shielding: Two problems exist: shielding target related backgrounds from the bremsstrahlung foil, and containing secondaries produced by the degraded primary beam according to standard guidelines. [7] [8]

A 0.1 radiation length target puts 10% of the primary energy into photons at 0 degrees, requiring that the photon showers and muons produced downstream be absorbed, Fig 12). The primary absorber is assumed to be the heavy slot collimators which should effectively absorb all the photon energy. A secondary, clean up, collimator would further reduce transmission of the showers at 0 degrees, while also absorbing shower secondaries produced from the degraded primary beam. The bremsstrahlung target will be interlocked so that only thin foils can interact with the beam.

The degraded primary beam has been tracked using TURTLE, (Figure 12). Electrons will be transported by the downstream quads without major losses, however the bending magnets will spread the beam which could produce secondary radiation sources when spray hits the vacuum pipes or other hardware upstream of the dump. Protection collimators (PC's) can be introduced into the beamline to absorb shower secondaries in a confined area. The first dumpline PC in front of the bend magnet chain will also be useful for this purpose.

Minimizing Backgrounds: The primary problem in minimizing backgrounds is to provide sufficient attenuation between the bremsstrahlung target and detector to remove as many high energy photons as possible. This will be accomplished using slit collimators whose opening is small enough to transmit the narrow stripe of beam while being opaque to shower secondaries. Slit collimators made from tungsten blocks can be polished optically flat and separated using shim spacers available in a continuous range of thicknesses down to 1 nm.[17] A sweeping magnet would remove μ's produced by the bremsstrahlung photons.

Radiation Hardness of Components: Present plans call for only two active components to be within the shielding: the bremsstrahlung target insertion mechanism and the primary collimator controls. Both of these components will be subject to radiation damage. The target controller can be located perpendicular to the beam direction target where fluxes from thin targets are low. The primary collimator motion can use servomotor systems which are not particularly sensitive to radiation. The encodermotor systems used at the Argonne APS linac contain one transistor in the encoder amplifier circuit which probably limits their operation to about $\sim$1000 Rads.

Request for Running Time, Space

Every attempt will be made to use parasite beam to debug the apparatus, and shielding using parasite beam time and other test beams. Nevertheless it would be desirable to have 15 shifts of primary user time for online alignment of components and data taking, with components as shown in Figure 8. Operating time with the Plasma Lens experiment would also be desirable. Operation with a streak camera would be desirable but should depend on the FFTB experimental program.

References

[1] Norem, J., Rev. Sci. Instrum., **62(6)**, (1991), 1464

[2] J. Norem, Proceedings of the 1988 Linear Accelerator Conf., Newport News, Virginia, (1988), p430

[3] Jenkins and White, *Fundamentals of Optics*, Fresnel Diffraction, McGraw-Hill (1957)

[4] H. A. Bethe, in Experimental Nuclear Physics Vol 1, E. Segre, ed., John Wiley and Sons Inc. New York, (1953), p166

[5] J. Litt and R. Muenier, Annu. Rev. Nucl. Part. Sci., **23**, 1, ('73)

[6] B. Rossi, High Energy Particles, Prentice-Hall Inc, Englewood Cliffs N. J., (1952)

[7] DOE Order 5480.11 Shielding Design Criteria, 12/21/88

[8] SLAC Memo from K. Crook, SM817, "Beam Containment Policy", 2/9/93.

[9] R. B. Palmer, Annu. Rev. Nucl. Part. Sci. **40**, 529, ('90)

[10] Seeman, J. T., Decker, F. J., Hsu, I., Young, C., 1991 Particle Accelerator Conference, San Francisco, Calif, May 6-9, (1991), 1734

[11] J. B. Rosenzweig, P. Schoessow, B. Cole, C. Ho, W. Gai, R. Konecny, S. Mtingwa, J. Norem, M. Rosing, and J. Simpson, Phys. Fluids B **2**, 1376, (1990)

[12] Chen, P., Phys. Rev. D, **46**, (1992), 1186.

[13] Schroeder, D. V., Stanford Linear Accelerator Center Report SLAC-371, SLAC, Stanford, CA, (1990)

[14] Proc. of the 1st TESLA Workshop, Cornell U, Ithaca, NY, CLNS 90-1029 (1990), ed H Padamsee.

[15] Proceedings of the International Workshop on Final Focus and Interaction Regions of Next Generation Linear Colliders, May 2-6 1992, SLAC Report SLAC-450, Stanford, CA

[16] F. Villa, (SLAC, private communication, 1991)

[17] Goodfellow Corporation, Malvern, PA 19355-1758

[18] R Lowrey, Rockwell Power Systems, Albuquerque NM (private communication).

[19] Hamamatsu Photonic Systems Corp, Park Ridge, IL 60068.

[20] R. E. Ruland, G. E. Fischer, Proceedings of the 2nd International Workshop on Accelerator Alignment, Hamburg, Germany, Sept 10-12, 1990. **and** Stanford Linear Accelerator Laboratory publication SLAC-PUB-5326 (1990)

[21] J. Buon, F Couchot, J. Jeanjean, F. Le Diberder, V Lepeltier, H. Nguyen Ngoc, J. Perez-y-Jorba, M. Puzo, and P. Chen, Nucl. Instrum. and Methods., **A306**, (1991), 93

[22] T. Shintake, Nucl. Instrum. and Methods, **A311**, (1992), 453

A beam profile monitor for small electron beams

APPENDIX A

J. Norem
High Energy Physics Division, Argonne National Laboratory, Argonne, Illinois 60439

(Received 23 January 1991; accepted for publication 6 February 1991)

Measurement of beam properties at the foci of high energy linacs is difficult due to the small size of the waists in proposed and existing accelerators (1 nm $-2\ \mu$m). This article considers the use of bremsstrahlung radiation from thin foils to measure the size and phase space density these beams using nonimaging optics. The components of the system are described, and the ultimate resolution, evaluated theoretically for the case of the Final Focus Test Beam (FFTB) at Stanford Linear Accelerator Center, is a few nm.

I. INTRODUCTION

The design of efficient linear colliders requires very small beams to produce high luminosities.[1] The small beams, in turn, require high precision and stability in all accelerator components. Producing, monitoring, and maintaining beams of the required quality has been, and will continue to be, difficult. This article describes a beam monitoring system that could be used to measure beam size and stability at the final focus of a beamline or collider.

The system consists of a bremsstrahlung radiator at the focus of the electron beam, a single sided collimator to produce a bremsstrahlung shadow, and a slit and detector system to measure the shape of the shadow edge.[2] In addition, sweeping magnets and shielding are required to disperse and absorb electron and photon backgrounds, Fig. 1. Dimensions are those assumed for the SLAC/FFTB system and are not critical. Other light sensitive detectors could be used instead of the streak camera. The sharpness of the shadow is inversely proportional to the size of the spot at the bremsstrahlung source. The optics of the system can be shown by plotting beam phase space at the focus, at the collimator and at the detector downstream, as shown in Fig. 2. By moving the detector slit back and forth it is possible to measure the shadow width, and hence the beam profile. Moving the primary collimator alters the initial x' values, thus the whole phase space density distribution, $\rho(x, x', y, y', t)$, can be measured. At the final focus of the SLAC/FFTB[3] or the JLC/ATF[4] the technique should give a resolution of a few nm and less than 1 psec, though the best resolution in time and space may be incompatible. The parameters of the proposed beamlines are shown in Table I.

The technique starts with the following advantages over other systems:[6] enormous signal brightness (bremsstrahlung intensity/emittance), simple analysis (using theory developed in 1815[5]), and detectors which are, in principle, blind to the most troublesome background. Implementation is complicated by the fact that the system must operate in or near the electron beam dump and in the presence of showers caused by collimators. It is assumed that a detailed design, including shielding, could be done after the rest of the system was specified.

II. COMPONENTS

Collimators can be made from commercially available metal mirrors, which are described in catalogues with a flatness of $< \lambda/40 \sim 14$ nm, and surface roughness of better than 1 nm.[7] Six invar mirrors with dimensions of $\sim$5–10 cm, optically polished to a few nm surface roughness, would cost about $4000.[8] The ideal shape of the primary collimator would be slightly convex with the front edge tangent to one side of the slit and the downstream edge tangent to the other side of the slit. With a 1 μm slit opening, this would imply a sagitta of about 1 nm, which is essentially flat. It is assumed that guard collimators would be larger, heavier, and perhaps water cooled, rough positioning ($\pm$ 100 nm) of these should be sufficient.

Rough positioning of guard collimators can be done with a number of commercially available systems, such the Nanomover sold by Melles Griot, which can set 20 kg loads with $\pm$100 nm resolution over 25 mm.[7] The primary collimator and final slit would have to be more carefully positioned, possibly to tolerances of $\pm$1 nm. Fine adjustment can be done with piezoactuators or Inchworm drives, sold by Burleigh, for motions of 0.1 nm to 10 μm or larger.[9] It is assumed that the collimators will each be controlled with three actuators, and the precision adjustment of these would be done in real time. Mirrors can be mounted to the structure in a number of ways, a compliant mount, such as pitch, might be desirable.

To examine the penumbra with high resolution, it is necessary to use a slit just before the convertor. A precollimator is inserted upstream of the open side of the slit to reduce shower backgrounds on it. It is assumed that Xe gas at 1 atm can be used as the Čerenkov radiator. With a refractive index $n = 1.000\,71$, the opening angle of radiation is 2.1°, and the minimum detectable electron energy is $\sim$ 12 MeV. This article assumes that the pair converter is U, 3.6 mm thick, and the Č radiator is 2 cm thick. In this geometry, electrons are efficiently used, as the Čerenkov source is inherently slitlike, and the slit on the streak camera may be unnecessary.

Time resolution within the bunch, using a streak camera, adds the requirement that the maximum amount of light be available for high resolution streak pictures. In the Argonne AATF, streak camera measurements have been done with 3×10^{10} electrons imaged at roughly unit mag-

 0034-6748/91/061464-04$02.00 © 1991 American Institute of Physics

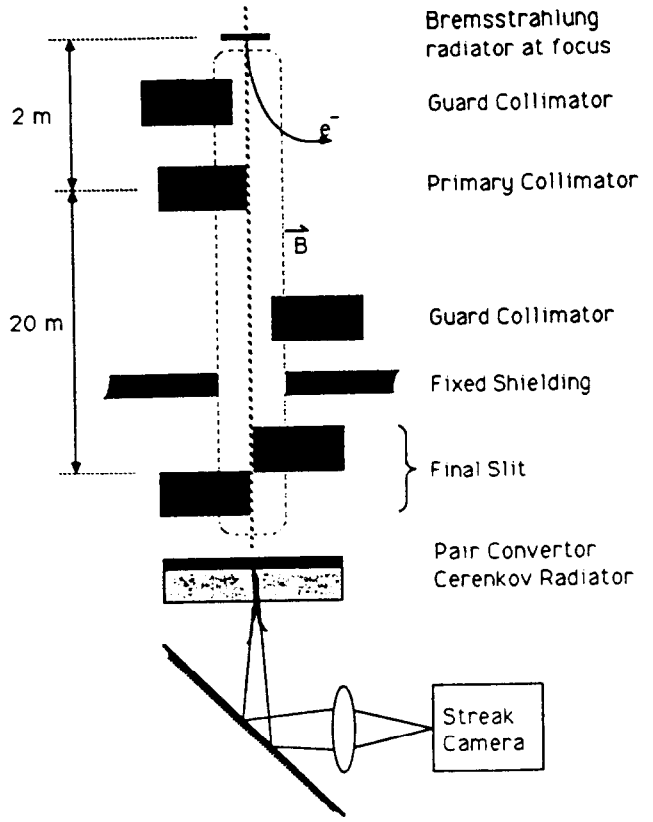

FIG. 1. The components of the monitor. The beam is defined by the primary collimator and measured by moving the final slit transverse to the beam.

nification on a slit set at about 100 μm, using 2 mm of Xe at atmospheric pressure, giving long, bright streaks.[10] For simple intensity measurements, shorter streaks should be sufficient, which should require $I_e \sim 8\times 10^7$ [e^- mm$_{Xe}$], with $I_e = n_e(l/L_R)\eta(\phi/\sigma_{x'})\Delta z$, where n_e is the number of electrons, l/L_R is the thickness of the bremsstrahlung radiator in radiation lengths, L_R, η is the number of electrons detected for one equivalent full energy photon on the detector, which is calculated by Monte Carlo and is roughly

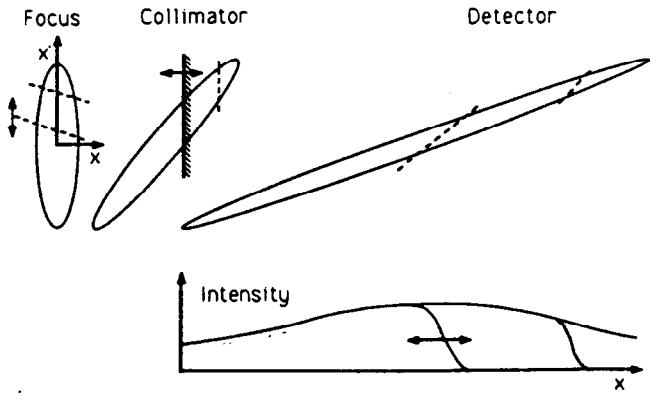

FIG. 2. Photon phase space of the system, not to scale. The collimator produces an edge which is measured downstream. A projection in x space shows the observed beam profile.

TABLE I. Parameters of test beams (Ref. 4).

	SLAC/FFTB	JLC/ATF
E, GeV	50	1.54
n_e	10^{10}	10^{10}
σ_x,m	1.0×10^{-6}	3.6×10^{-6}
ϵ_y,m	4×10^{-11}	10^{-11}
β_y,m	10^{-4}	8×10^{-5}
σ_y, m	6.3×10^{-8}	2.9×10^{-8}
σ_z, m	5×10^{-4}	8×10^{-4}
f, Hz	10	25

1–10 depending on the detector, $\phi/\sigma_{x'}$ is the acceptance of the detector divided by the divergence of the beam, and Δz is the length of Čerenkov radiator. The bremsstrahlung radiator should have a small radiation length and its thickness should be $\sim \beta$, to stay within the waist.

Commercial streak cameras have a resolution of 0.6–2 ps.[11] The streak camera is required for time resolved images, but almost any ionization detector (film, scintillator, ion chambers) could be useful for profile or stability measurements. Čerenkov radiators are a good way of hardening the detector, which is highly desirable. At the highest resolution, the system will probably not produce enough light for time resolved images.

III. LIMITATIONS

The ultimate resolution of this system is limited by Fresnel diffraction. If the intensity of diffraction pattern on a screen is given by $F(y)$, the width of the pattern is a function of

$$y = v\sqrt{\frac{b\lambda(a+b)}{2a}}, \tag{1}$$

which gives the dimensions in terms of v, the dimensionless variable used to evaluate the Fresnel integrals, $a = 20$, $b = 2$ m, from Fig. 1, and λ, the wavelength of the photons.[5] The resolution of the system is determined by incoherently adding the diffraction images produced by the bremsstrahlung spectrum as seen by the detector. The acceptance of the detector has been evaluated by means of a Monte Carlo program that generates a bremsstrahlung spectrum, computes pair production and subsequently evaluates multiple scattering.[12] The detected spectrum, which depends somewhat on position and angle cuts, is shown in Fig. 3. This article defines a resolution function as the derivative of this sum of diffraction images and this is shown in Fig. 4. This curve is the effective shape of a beam at the bremsstrahlung radiator in the limit of a zero width slit at the detector, assuming the dimensions given in Fig. 1. The resolution is nongaussian. Assuming a gaussian for the equivalent resolution of a diffraction image, one finds $\sigma_{y[\mathrm{nm}]} \sim 15 E_{[\mathrm{GEV}]}^{-1/2}$; however, high energy photons are weighted strongly.

The beam will self focus in the radiator. Magnetic fields $B_\phi \sim \mu_0 I/4\sqrt{2\pi}\sigma_x \sim 50$ T will produce deflections, $\theta_{f,\max} \sim B_\phi l/B\rho = 0.0002$, which will be comparable to multiple scattering of the primary beam in the radiator,

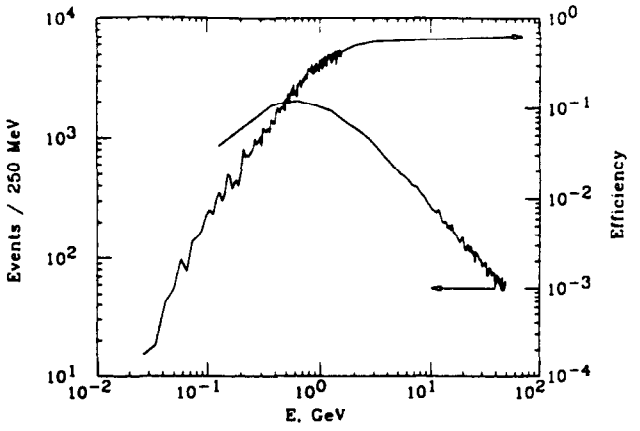

FIG. 3. Monte Carlo simulation of the detected photon energy spectrum and detection efficiency for the SLAC/FFTB beam, with electron angle $\theta_e < 2°$.

$\theta_{ms} = 0.014/p\sqrt{l/L_R} = 0.000\,12$, and smaller than the divergence of the 60 nm beam, $\sigma_{x'} \sim 0.0006$. This article assumes $\mu_0 = 4\pi \times 10^{-7}$, I is the beam current, $l = -0.1$–0.6 mm, $L_R = 3.6$ mm, $n_e = 10^{10}$, $\sigma_z = 1$ mm, $\sigma_x = 1$ μm and beam momentum $p = 50$ GeV/c, with Bρ $= 3p$. The field B_ϕ will cause synchrotron radiation, with photons of 100 MeV or less; however, the total energy lost into this radiation will be much smaller than into bremsstrahlung. Self focusing and multiple scattering can be minimized with a thinner primary radiator, which may be desirable under some circumstances. The angular distribution of bremsstrahlung photons relative to the electron beam direction, is roughly m_e/E_e, where m_e and E_e are the electron mass and initial energy.[12] Self focusing, multiple scattering, and angular effects primarily introduce diffusion in the x' dimension of phase space at the focus (see Fig. 2) and these effects can be corrected.

Almost comparable resolution can be obtained for the JLC/ATF Final Focus Test [4] if the primary collimator is moved within 0.5 m of the final focus. Since the expected spotsize is 30 nm, coming from a β of 80 μm, high resolution is desirable. The spectrum of detected photons is roughly flat, thus the average photon energy is a larger fraction of the maximum energy. The target thickness and the beam energy cause problems. The target must be thin to fit within the waist of the beam, and this reduces the intensity of the bremsstrahlung photons. The low energy of this beam, 1.54 GeV, permits the primary electrons to be steered away from the photon beam in a smaller distance, but causes large multiple scattering, which will detectably increase both the beam divergence and the beam itself in a 20 μm radiator thickness.

Fully utilizing the theoretical resolution of this system will require that the collimators must be mounted on a vibration free surface.[13] Both active and passive vibration damping systems might be considered. The problem is, however, similar to the vibration sensitivity of the final quads in the line, and should probably be solved the same way. The passive damping used on the final quads before the focus should be sufficient to produce useful measurements. Slow drifts and low frequency oscilations will probably require that measurements be taken with a few pulses and collimator positions be maintained using active corrections.

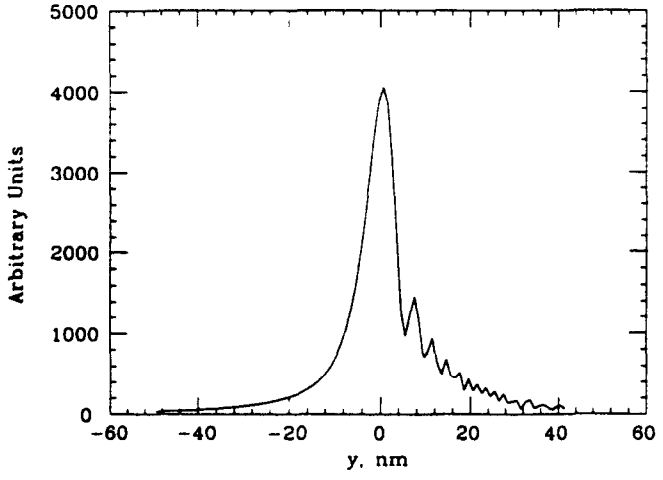

FIG. 4. The resolution function, defined as the derivative of the diffraction intensity at the bremsstrahlung radiator.

IV. BACKGROUNDS

The system should be blind to synchrotron radiation, which is troublesome because it is produced by the beam with very small emittance near the final focus. Although the streak camera detects visible and near UV, direct synchrotron radiation from the beam in magnets, plasmas or the primary radiator would be blocked by the bremsstrahlung radiator and pair converter.[14] The optics of the streak camera can be made light tight.

The primary means of discriminating between signal and shower electrons is that the brightness of the signal should be much higher than that of the showers, which can be magnetically dispersed in two dimensions. In addition, timing can be used to separate direct photon paths from indirect shower paths

The environment downstream of the final focus will be inhospitable to precision equipment. Mechanical, optical and electrical components should be tested to make sure they will function in the high radiation environment.

V. DISCUSSION

This article outlines the components and limitations of a system designed to measure beam profiles for high energy colliders and test beams; a particular goal of this design was time resolution within the bunch. The beam layout must minimize shower contamination of the bremsstrahlung signal and vibration of components.

The overall dimensions and components of this system can be adapted to the priorities of the measurement program. Time resolved measurements of plasma focused beams will require time resolution from a streak camera. Obtaining the ultimate resolution in phase space densities, on the other hand, will require much smaller slit openings

and more sensitive detectors. Likewise the linear dimensions of the system can be adapted to the required shielding.

It is generally assumed that data will be taken by scanning the detector slit across the image in the y direction and building up the beam image over a number of beam pulses. It should, however, be possible to produce a profile measurement in one accelerator pulse if the detector slit is inclined slightly with respect to the primary collimator. If the dimensions of the electron shower are small compared with the overall size of the beam, positions in y will be correlated with different initial x' values. Thus a scan along x at the detection slit would be equivalent to a scan along y. This extension would require that the initial phase space density was uncorrelated in y and x', or the technique could be used to look for these correlations.

The system can be extended to higher energies; however, beam focusing in the bremsstrahlung radiator becomes more severe as the beam size is reduced and the current is increased. Inverse Compton scattering from intense laser pulses can be used instead of bremsstrahlung to produce high energy photons, which can be examined using the method described here. To efficiently use the laser photons, the laser pulse length must be shorter than the length of the beam waist, which for high energy designs is generally less than 100 μm, or 300 fs. The lasers needed to produce the high photon density required are expensive.

ACKNOWLEDGMENTS

P. Schoessow of ANL produced EGS4 calculations of showers in slits, and G. Fischer of SLAC has provided information on vibration and surveying techniques. Work supported by the U. S. Department of Energy, Division of High Energy Physics, Contract No. W-31-109-ENG-38.

[1] R. B. Palmer, Annu. Rev. Nucl. Part. Sci. 40, 529 (1990).
[2] J. Norem, Proceedings of the 1988 Linear Accelerator Conf., Newport News, Virginia (1988), p. 430.
[3] K. Oide, Proc. 1989 Particle Accelerator Conf, Chicago (1989), p. 1319
[4] K. Oide, Proceedings of the First Workshop on Japan Linear Collider (JLC) KEK (Japan), October 24–25 (1989), p. 13.
[5] F. A. Jenkins and H. E. White, *Fundamentals of Optics* (McGraw-Hill, New York, 1957), Chap. 18.
[6] J. Buon, Particle Accelerators 31 IV, 1247 (1990).
[7] Melles Griot, Irvine CA 92714.
[8] R. Lowrey, Rockwell Power Systems, Albuquerque NM 87107 (private communication).
[9] Burleigh Instruments Inc., Fishers, NY 14453.
[10] J. B. Rosenzweig, P. Schoessow, B. Cole, C. Ho, W. Gai, R. Konecny, S. Mtingwa, J. Norem, M. Rosing, and J. Simpson, Phys. Fluids B 2, 1376 (1990).
[11] Hamamatsu Photonic Systems Corp., Bridgewater, NJ 08807.
[12] H. A. Bethe, in *Experimental Nuclear Physics*, edited by E. Segre (Wiley, New York, 1953), Vol. 1, p. 166.
[13] R. E. Ruland and G. E. Fischer, Proceedings of the 2nd International Workshop on Accelerator Alignment, Hamburg, Germany, Sept. 10–12, 1990 and Stanford Linear Accelerator Laboratory publication SLAC-PUB-5326 (1990).
[14] C. Field, Proceedings of the 1989 IEEE Particle Accelerator Conference, Chicago, IL, March 20–23 (1989), p. 60.

HAMAMATSU

FEMTOSECOND STREAK CAMERA FESCA-500

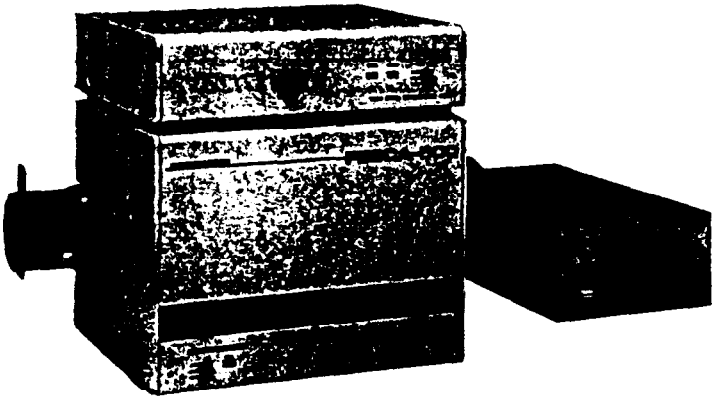

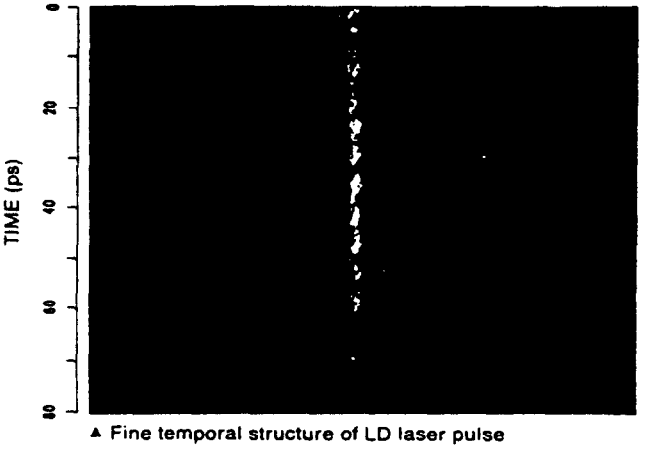

▲ Fine temporal structure of LD laser pulse

Achieves 600 femtosecond time resolution! Simultaneous measurement of light intensity, time and position (or wavelength).

The FESCA-500 is an ultrafast streak camera which has time resolution as fast as 600 femtoseconds (0.6 picosecond). In the past, ultrafast phenomena occuring within one picosecond have been measured by indirect mesurements such as an autocorrelation method.
The FESCA-500, however, enables the realtime direct measurement of light phenomena of less than one picosecond. The FESCA-500 can analyze the process of energy relaxation and dynamics of chemical reaction in the femtosecond region in combination with femtosecond pulsed laser.

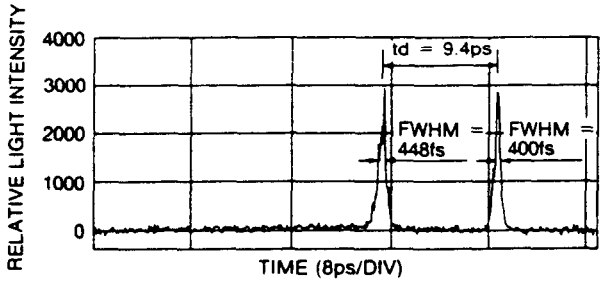

▲ Measurement example (CPM laser)

FEATURES

- **600 femtosecond (0.6 picosend) time resolution.**
- **Two measurable spectral regions. (200~850nm, 300~1060nm)**
- **Simultaneous measurement of light intensity, time and position (or wavelength).**
- **Optional exclusive readout system. (Realtime processing and analysis of streak image.)**

APPLICATIONS

- **Research for the process of energy relaxation of quantum well semiconductor.**
- **Research for dynamics of chemical reaction in the femtosecond region.**
- **Research for dynamics of ultrafast laser diode, ultrafast optical logic devices, etc.**
- **Diagnosis of femtosecond laser.**
- **Optical solition.**

SPECIFICATIONS

- **Streak Tube N3373 or N3373-02**

Photocathode/window material
N3373 ..... Multi-alkali/UV glass
N3373-02 ..... Ag-O-Cs/kovar glass
Spectral response characteristics
N3373 ..... 200 ~ 850nm (S-20)
N3373-02 ..... 300 ~ 1060nm (S-1)
Useful photocathode size ..... 3mm dia.
Phosphor screen P-20
Useful phosphor screen size ..... 15mm dia.
Image magnification 3.3
MCP gain ..... more than 10^3
Spatial resolution
(on the center of photocathode) ..... 75lp/mm (typ.)

- **Fast Single Sweep Unit**

Temporal resolution (at the fastest speed range)
..... better than 700fs (600fs typ.)
Streak time/full screen (10mm)
..... 60ps, 200ps, 500ps, 1.2ns
Trigger jitter ..... less than ± 30ps
Trigger delay (at the fastest speed range) .... 20ns (typ.)
Dynamic range (at the fastest speed range)
..... more than 1:40
Repetitive frequency ..... max. 1 KHz

- **Input optics**

Item \ Name	UV type	Visible light type		Infrared type	
	A1976-01	A1974	A1975	A1974-01	A1975-01
Spectral transmittance (nm)	200~1600	400 ~ 900		400 ~ 1600	
Image magnification	1:1	1:1	3:1	1:1	3:1
Effective F number	4.5	1.2	4.5	1.2	4.5
Overall length (mm)	98.2	190	190	159	200

- **Mainframe**

Gating method ..... MCP or shift simultaneous gating
Gate time ..... 200ns to continuous
Gate extinction ratio ..... more than $1:10^5$
Line voltage ..... 100/117/220/240 VAC, 50/60Hz
Power comsumption ..... Approx. 200VA

OPTIONS

- **Pin diode head C1083**
- **Delay unit C1097**
- **Cooled CCD camera C3140**
- **Streak camera readout system**
- **Video monitor**

DIMENSIONAL OUTLINE (unit:mm)

- **Mainframe (approx. 35kg)**

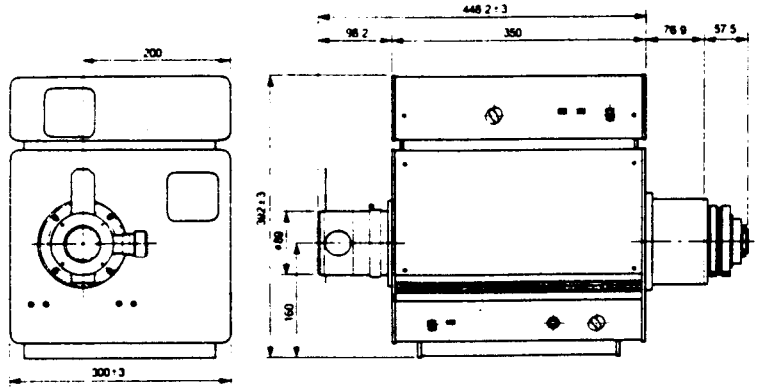

- **Power supply unit (approx. 10kg)**

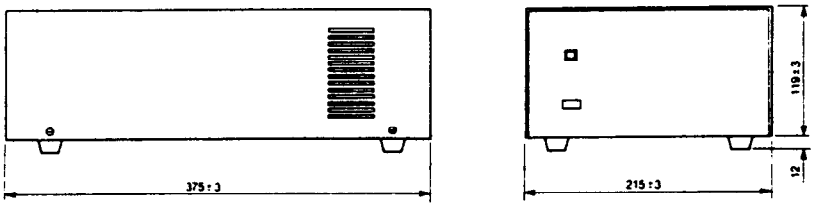

• Specifications and external appearance are subject to change without notice.

HAMAMATSU

HAMAMATSU PHOTONICS K.K., System Division
812 Joko-cho, Hamamatsu City, 431-32, Japan, Telephone: 0534/35-1562, Fax: 0534/35-1574, Telex: 4225-187,

U.S.A.: Hamamatsu Photonic Systems Corporation: 360 Foothill Road, Bridgewater, N.J. 08807-0910, U.S.A., Telephone: 201-231-1116, Fax: 201-231-0852
W. Germany: Hamamatsu Photonics Deutschland GmbH: Arzbergerstr. 10, D-8036 Herrsching am Ammersee, West Germany, Telephone: 08152/375-0, Fax: 08152/2658, Telex: 527731
France: Hamamatsu Photonics France, Zone ORLYTECH - Bât. A3 - Allée du Cdt Mouchotte, 91550 PARAY VIEILLE POSTE, Telephone: (1) 49 75 56 80, Fax: (1) 49 75 56 87, Telex: HPF631895F
United Kingdom: Hamamatsu Photonics UK Limited: Lough Point, 2 Gladbeck Way, Windmill Hill, Enfield, Middlesex EN2 7JA, England, Telephone: 01-367-3560, Fax: 01-367-6384
Telex: 927817 PHOTON G
North Europe: Hamamatsu Photonics Norden AB Kanalvägen 20, S-194 61 Upplands Väsby, Sweden, Telephone: 0760/32190, Fax: 0760/94567

Catalog No.: TV-178
JUL/89
CR-3000 Printed in Japan

STS-2

Portable Very-Broad-Band Seismometers

G. Streckeisen, AG
Dättlikonerstraße 5
CH-8422 Pfungen
Switzerland

Quanterra, Inc.
Very-Broad-Band Seismological Instrumentation
325 Ayer Road
Harvard, MA, USA 01464
Tel: 508-772-4774
FAX: 508-772-4645

The information in this document has been reviewed and is believed to be reliable. Streckeisen, AG and Quanterra, Inc. reserve the right to make changes at any time and without notice to improve the reliability and function of the products described herein.

No part of this publication may be reproduced, stored in a retrieval system, or transmitted, in any form or by any means, electronic, mechanical, photocopying, recording, or otherwise, without the prior written permission of Streckeisen AG, and Quanterra, Inc.

Copyright ©1993, Streckeisen, AG, and Quanterra, Inc.

1.0 Introduction

The Streckeisen, AG, STS-2 seismometers are sensitive, remotely-controlled, wide-bandwidth seismic sensors. Their high dynamic range and stable transfer characteristics make them ideal for a wide range of applications. The second-generation STS-2 complements the high-performance STS-1 seismometers that have been produced since 1976.

The STS-2 is designed for quick and simple installation, wide temperature range operation, and secure transport, while resolving minimum earth noise levels over the frequency range equivalent to and exceeding traditional long- and short-period instruments. Special shielding is normally not required to resolve levels 10--30 times below the limit of World-Wide Standard Seismographs.

Like the STS-1, the STS-2 is an electronic force-feedback sensor that provides an output signal proportional to ground velocity over a broad range. Similarly, the STS-2 also employs the astatic leaf-spring suspension (Wielandt and Streckeisen, *BSSA*, 1982). The flat velocity response, derived within the STS-2's feedback loop, provides a high short-period saturation level, better than 0.1 g at 10 Hz.

The STS-2 uses 3 identical obliquely-oriented mechanical sensors, rather than the traditional separate orthogonal vertical and horizontal sensors. In addition to benefits in standardization of manufacturing, the tri-axial design guarantees that horizontal and vertical components are matched as closely as possible. Standard vertical and azimuthally orthogonal horizontal outputs are derived electrically rather than mechanically, making the seismic output signals appear to the user as those of a conventional three-component seismometer.

The main features of the STS-2 compared to the STS-1 are:

- Bandwidth suitable for general-purpose teleseismic and regional recording: corners at 120 sec and >50 Hz.
- Smaller size and lower power consumption.
- The STS-2 is a single sealed, all-metal tri-axial sensor package that includes all essential electronics.
- Quick installation and setup using no special tools or instruments. Setup features include a built-in bubble level, an automatic recentering circuit, and conversion to 1-second free period operation to reduce transient response time during centering and levelling adjustments.
- Wide temperature range -- minimum ±10°C without recentering.
- Robust transport locking mechanism actuated by rotation of an externally-accessible screw for each sensor without opening the sealed sensor package.
- Enhanced resolution of short periods using a capacitive displacement transducer.
- Stronger electromagnetic feedback giving higher dynamic range in the mid-frequency range of 0.1--10 Hz, where local and regional events generate high peak amplitudes.
- No external pressure shielding required for most broad-band and long-period applications.

1.1 General Description

1.1.1 Physical

Three identical sensors with electronics and power conditioning are mounted in a cylindrical package approximately 235 mm in diameter and 260 mm high. Power, logic-level control signals, and calibration signals enter the STS-2 on a single 18-conductor cable that is also used to deliver the 3-component differential output signal and single-ended mass position signals. The standard 18-conductor cable is 3 meters long, and is terminated in a 'host-box'.

Three threaded mounting feet allow levelling of the seismometer package. A screw to actuate the transit lock of each sensor is accessible along the edge of the base ring. The top and bottom of the STS-2 have aluminum covers that are gasketed to the base plate.

The STS-2 is vacuum-tight. The construction is further designed to minimize the distortion of the package by barometric pressure changes by isolating the top and bottom covers from the massive base plate, in a way similar to the isolation of a seismograph pier from its surrounding building. The top and bottom covers are secured to the base plate with compliant O-rings, allowing the covers to compress without stressing the entire package. The sealed construction and massive metal base plate provide thermal isolation and inertia.

Since all 3 sensors are mutually aligned by mounting to a common frame and the complete package is factory-calibrated using a standardized 3-dimensional shake table, the STS-2 eliminates some common causes of installation and calibration error. It it necessary to orient and level only a single package in the field. It is not necessary to open the STS-2 package, or to individually adjust and orient each sensor.

1.1.2 Feedback System

Electronic force feedback permits a near infinite variety of seismometer responses. Feedback systems can be derived to optimize individual parameters such as saturation level, sensitivity, bandwidth, or frequency response. The feedback system for the STS-2 is chosen to be a compromise suitable for most general applications.

The STS-2 feedback system is basically identical to that of the STS-1/VBB (Wielandt and Steim, *Annales Geophysicae*, 1986, although the feedback is stronger at short periods, improving linearity and extending the high-frequency flat-velocity frequency response. The low-frequency -3 dB corner of the STS-2 is set at 120 s.

No filters, which limit dynamic range, are used to derive the velocity-proportional output; the STS-2 feedback system delivers velocity directly from the feedback loop. The output stage of the feedback electronics for each component provides a high-level (40 V p-p, max) differential output signal, suitably for direct connection to a high-resolution A/D converter, such as the Quanterra *Q680*.

1.1.3 Output Signals

The raw electrical output of each of the STS-2's obliquely-mounted sensors contains both vertical and horizontal components of motion. These signals are electrically summed within the STS-2's electronics to provide standard vertical and horizontal output signals. Cross-coupling between components is suppressed electrically during manufacturing, rather than by depending on the mechanical adjustments. Independent single-ended "boom position" signal outputs are also available from each sensor. These signals may be monitored externally during setup or routinely during operation to determine proximity to the limit of operation.

1.1.4 Orientation

The orthogonal output signals are factory-adjusted to represent motions in the X, Y, Z axes within an accuracy of 1% (±0.6°) at 6 s period. Physical orientation of the STS-2 by the user requires determination at installation of only 2 parameters: the verticality and azimuth of the package. Each STS-2 package is equipped with an integral bubble level and orienting rod to allow rapid, properly-oriented installation without special tools.

1.1.5 Calibration

The effective free-period and damping of each channel of every STS-2 is adjusted at the factory within ±1% of the nominal values. The frequency response of the closed-loop system is simple and familiar to seismologists. The output of the STS-2 is equivalent to a 120-sec electromagnetic seismometer coupled to a high-frequency galvanometer.

1.1.6 Standard and Low-Power Versions

A low-power version is available as a no-cost option that is optimized for field-portable applications, requiring typically <1W average. Some minor degradation, typically 6dB, of low-frequency (10 mHz) and high-frequency (10 Hz) noise levels may be expected. In many portable applications, ambient seismic noise, and not instrumental self-noise, limits performance.

1.1.7 Electrical Inputs

The STS-2 comes supplied with a 3-m interface cable that is terminated at the sensor end in a seismometer connector and is terminated at the other end in a 'host box'. Power, control, output signals, and calibration signals are accessible at the host box. The host box also contains DC/DC converters, input protection circuits, and other signal distribution.

1.1.7.1 Calibration Current

The STS-2 provides inputs to separate calibration coils to allow excitation of the STS-2 with arbitrary calibration currents. The return leg of all calibration coils are tied together.

1.1.7.2 Control Inputs

Logic-level inputs are provided on the STS-2 to control: monitor-signal selection (trigonal "boom-position" or raw sensor outputs), mass recentering, and selection of low-frequency corner period. The STS-2 can automatically zero the boom position on receipt of an autozero command or by pressing the "AUTOZERO" push-button. The automatic cycle requires about 30 sec.

To reduce installation time, during the autozero cycle, the STS-2 changes its low-frequency corner period from 120 s to 1 s without exciting the seismometer's impulse response that can require 10--20 minutes for complete decay. When the cycle is complete, the 120 s corner is restored, also without exciting the sensor impulse response.

1.1.7.3 Power

The STS-2 contains an isolating, regulated DC/DC converter. Primary power is protected against polarity reversal overvoltage. Primary DC operating voltage is 10-30,VDC. Power consumption for the standard version is 1.8W.

1.1.8 Installation

A double styrofoam box to provide isolation against rapid temperature changes and air currents improves long-period noise level. Satisfactory results may be obtained using only a single box. We have found that in a typical seismic vault with still air and relatively constant temperature, an STS-2 covered by a single box without special sealing can resolve minimum earth noise levels to nearly 50 sec period. Operating in this mode, 3-component long-period narrow-band (25-35 sec peak) recordings by STS-1 and STS-2 seismometers are virtually identical.

Applications requiring highest performance may use an external pressure-isolating cover with a time constant on the order of a few hours. A vacuum-tight external cover is not required or recommended.

1.2 Specifications

1.2.1 General

1.2.1.1 Principle of operation

Force Balance

1.2.1.2 Mechanical sensors

Three identical inertial pendula oriented 120° apart.

1.2.1.3 Primary output signals

Vertical (Z) and 2 orthogonal horizontal (X,Y), broad-band velocity

1.2.1.4 Size

1 cylindrical package approx. 235 mm in diameter, 260 mm high.

1.2.1.5 Weight

13 kg, including host box.

1.2.1.6 Environmental protection

Vacuum-tight, low-stress construction.

1.2.2 Electro-mechanical

1.2.2.1 Output level

40 V p--p, differential. (±20V)

1.2.2.2 Generator constant

2 x 750 V-sec/m

1.2.2.3 Response

Corners: 120 s (2-pole) and >50 Hz, flat velocity:

1. At frequencies below 1 Hz, the response may be considered to be a 2-pole Butterworth high-pass to velocity (damping 0.707) with a corner period of 120 s. The response $T(f)$ to ground displacement at frequency f is therefore expressed by:

$$T(f) = \frac{2\pi i f G_0}{1 - \frac{2if_0h}{f} - \left(\frac{f_0}{f}\right)^2}$$

where: G_0 is the generator constant 1500 Vs/m, f_0=0.00833 Hz, and h=0.707.

2. From 1-10 Hz, the velocity response is flat ±0.15dB. The group delay is 4±1 msec.

3. The "flat"-velocity response extends somewhat beyond 50 Hz. However, the overall response at high frequencies depends not only on the seismometer, but also on its coupling to the ground. While coupling may influence significantly the amplitude and phase, the influence on group delay is small. The group delay observed on a shake table is a nearly-constant 3±1 msec at frequencies between 10 and 50 Hz. The amplitude response is typically flat within ±1.5dB over this range.

1.2.2.4 Electronic Self-noise

Approximately 6 dB below USGS Low-Noise-Model 0.008 Hz--10 Hz.

1.2.2.5 Clip Level

±13 mm/sec velocity, equivalent to the following accelerations:

Frequency	p-p Acceleration
10 Hz	0.167 g
1 Hz	0.0167 g
0.1 Hz	0.00167 g
0.03 Hz	5.5×10^{-4} g

1.2.2.6 Dynamic Range

Intrinsic dynamic range as a function of frequency is the interval between clip level and self-noise. Actual dynamic range is the interval between clip level and minimum ambient seismic noise. Typical maximum actual dynamic range exceeds 140 dB.

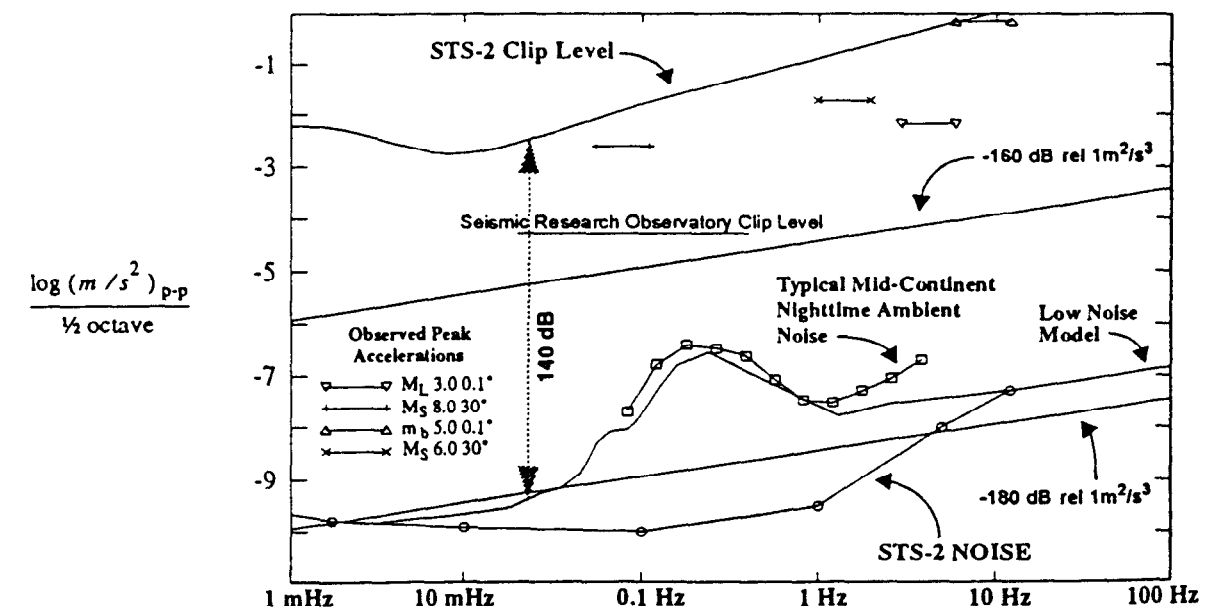

1.2.2.7 Parasitic resonance of main spring

Vertical >140 Hz. Horizontal >80 Hz.

1.2.2.8 Power

1.8W 10-30 VDC, standard-power version. 1W typical, low-power

1.2.2.9 Temperature range

Operating, full specifications: 0-40°C. Range without mass recentering ±10 °C. Extended operating and recentering range available.

1.2.2.10 Boom centering

Automatic on external command, push-button or logic-level.

1.2.2.11 Connectors

Watertight 18-pin circular on seismometer. MS3106 24-pin MIL-style connector on host box.

1.2.2.12 Calibration input

Calibration coil constant 0.002 g/mA (oblique). 50 mA max current. 30 ohms.

A Profile Monitor for Small Electron Beams

J. Norem*
Argonne National Laboratory
Argonne, IL, 60439, USA

June 6, 1991

1 Introduction

The design of efficient linear colliders requires very small beams to produce high luminosities [1]. The small beams, in turn, require high precision and stability in all accelerator components. Producing, monitoring and maintaining beams of the required quality has been, and will continue to be, difficult. This note describes a beam monitoring system which could be used to measure beam size and stability at the final focus of a beamline or collider.[2] The immediate use for this system is, however, examining the final focus spot at the SLAC/FFTB and JLC/ATF.

The system, Figure 1, consists of a Bremsstrahlung radiator at the focus of the electron beam, a single sided collimator to produce a bremsstrahlung shadow, and a slit and detector system to measure the shape of the shadow edge.[2] In addition, sweeping magnets and shielding are required to disperse and absorb electron and photon backgrounds. The linear dimensions are not critical. Any light sensitive detector could be used including a streak camera. The sharpness of the shadow is inversely proportional to the size of the spot at the bremsstrahlung source. The optics of the system can be shown by plotting beam phase space at the focus, at the collimator and at the detector downstream, also shown in Fig. 1. By moving the detector slit back and forth it is possible to measure the shadow width, and hence the beam profile. Moving the primary collimator alters the initial x' values, thus the whole phase space density distribution, $\rho(x, x', y, y', t)$, can be measured. At the final focus of the SLAC/FFTB [3] or the JLC/ATF[4] the technique should give a resolution of a few nm and less than 1 psec, though the best resolution in time and space may be incompatible. The parameters of the proposed beamlines are shown at right.

This note is essentially a progress report which describes the method and a proposed installation at the SLAC/FFTB in as much detail as possible. A possible application of the method to the KEK/ATF is also considered in somewhat less detail.

*Work supported by the U. S. Department of Energy, Division of High Energy Physics, Contract W-31-109-ENG-38.

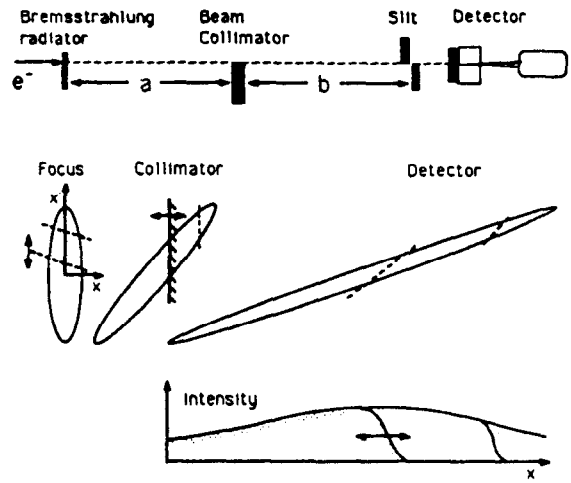

□ Figure 1, Basic layout, phase space of the system.

2 Requirements

The following table shows the parameters of the SLAC/FFTB and the JLC/ATF. These beamlines produce roughly similar spotsizes, although the beam energies are quite different.

	SLAC/FFTB	JLC/ATF
E, GeV	50.	1.54
n_e	$1-3\cdot10^{10}$	10^{10}
ϵ_x, m	$3\cdot10^{-10}$	10^{-10}
β_x, m	0.005	0.014
σ_x, m	$1.2\cdot10^{-6}$	$3.6\cdot10^{-6}$
$\sigma_{x'}$	$2.4\cdot10^{-4}$	$2.6\cdot10^{-4}$
ϵ_y, m	$4\cdot10^{-11}$	10^{-11}
β_y, m	10^{-4}	$8.\cdot10^{-5}$
σ_y, m	$6.3\cdot10^{-8}$	$2.9\cdot10^{-8}$
$\sigma_{y'}$	$6.3\cdot10^{-4}$	$3.5\cdot10^{-4}$
σ_z, m	$5.\cdot10^{-4}$	$5.\cdot10^{-4}$
f, Hz	$10-30$	25
$P_{e,max}$,W	2400	16

Jitter in the beam is experimentally found to be $\sim 0.2\sigma$, exclusive of what is introduced in the final focus line, so measuring jitter would require measurements on the order of 12 nm.

Both the SLAC and KEK diagnostic requirements are similar. Ideally one wants to measure the electron phase space distribution as directly and completely as possible on every pulse. Other requirements include good resolution in x and y, some resolution in z, equal response to $e^{+/-}$ and flat or round beams, sensitivity to beam jitter, ability to measure focal position (not straightforward in a system which sees only parts of phase space), stable mechanically to low frequencies, and compatible with beam power and beam and plasma backgrounds. In addition it would be useful to be able to examine systems that produce crab crossing and other specialized beam exotica.

The primary alternatives to this system are those proposed by P. Chen / J. Buon,[5] which analyses the angular distributions of ion recoils to determine the aspect ratio of the electron bunch, and a system proposed by Shintake,[6] which considers the intensities of compton backscattered photons from standing waves. The proposed system would be faster and higher precision than the other systems, providing more direct measurements of the original phase space distribution and such effects as jitter in the final spot. An additional feature of the proposed system is that the range of spotsizes over which it operates should be larger than the alternatives.

Under some circumstances it may be desirable to eliminate the bremsstrahlung radiator and replace this with a photon target from a laser beam. This would eliminate the multiple scattering and focusing of the beam due to plasma lens effects, and the production of synchrotron radiation associated with the focusing. The high power laser would be an expensive addition, however.

3 Operation

The operation the system for normal profile measurements should be straightforward. Scans of the beam at the detector should translate directly into profile measurements $\rho(y)$ at some value of y', and different values of y' selected by changing the position of the primary collimator. Similar measurements can be made in the x direction to generate a complete picture of $\rho(x, x', y'y')$. Measurements of y parameters can be measured simultaneously at different x values with specialized collimators and detectors, if required. Streak camera measurements can be used to provide some information on the z dimension of the bunch, however this will probably not be useful at the highest resolutions in x, y, since the narrow slit settings required will produce low photon fluxes into the streak camera.

It is somewhat difficult to determine the actual focal position of the beam since this system only sees roughly horizontal slices of the phase space at the focus. The measurement can be made by moving the primary collimator by a large distance $2a\sigma_{y'} \sim 4$ cm, measuring the position of the mean of of the penumbra at two points and extrapolating back to the focus. the error on the focal position is then $\Delta z = \sqrt{2}\delta y/\sigma_{y'} \sim 140\mu \sim \beta_y^*$, where $\delta y = 100$ nm is the measurement error. This is diagramed in Figure 2.

Although the most straightforward measurement is taken by scanning the detector slit across the image in the y direction and building up the beam image over a number of beam pulses, it should be possible to produce a profile measurement in <u>one</u> accelerator pulse if the detector slit is twisted slightly with respect to the primary collimator. If the dimensions of the electron shower are small compared with the overall size of the beam, positions in y will be correlated with different initial x' values. Thus an x profile at the detection slit would be equivalent to a scan along y. This requires that the initial phase space density was uncorrelated in y and x' and the technique could be used to look for these correlations.

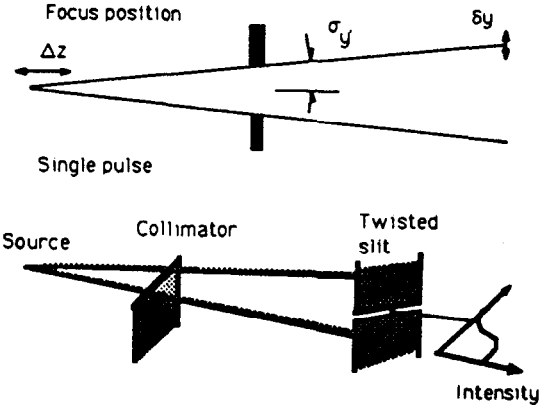

□ Figure 2. Focus position measurement and twisted slits.

3.1 Resolution

A number of processes limit the resolution of this system, depending on geometry, and the beam properties. In practice these terms will all be convolved together, with one term dominating. The individual items are outlined below:

3.1.1 Fresnel Diffraction

The ultimate resolution of this system is limited by Fresnel diffraction.[7] If the intensity of diffraction pattern on a screen is given by $F(y)$, the width of the pattern is a function of

$$y = v\sqrt{\frac{a\lambda(a+b)}{2b}}, \qquad (1)$$

which gives the dimensions of diffraction patterns on a screen in terms of v, the dimensionless variable used to evaluate the Fresnel integrals, and $a = 30$, $b = 30$ m, and λ, the wavelength of the gamma's.[7]. The resolution of the system is determined by incoherently adding the diffraction images produced by the bremsstrahlung spectrum as seen by the detector. The acceptance of the detector has been evaluated by means of a short monte carlo program which generates a bremsstrahlung spectrum, computes pair production and subsequently evaluates multiple scattering.[8] The detected FFTB spectrum, which depends somewhat on position and angle cuts, is shown in Fig. 3 for minimum detected electron energy of 15 MeV and maximum angle of 2°. This note defines a resolution function as the derivative of this sum of diffraction images and this is shown in Fig 4, for the highest resolution possible with the SLAC line. This curve is the effective shape of a beam at the bremsstrahlung radiator in the limit of a zero width slit at the detector. The resolution is nongaussian and $\delta x, y \sim E_\gamma^{-1/2}$, so high energy photons contribute most to the resolution.

The highest resolution is obtained by moving the collimator as close as possible to the final focus as possible, however the constraints of disposing of the high energy beam limit this dimension. More reasonable geometries are used in fig 5 and 6 to calculate realistic resolution functions for the SLAC and KEK beamlines.

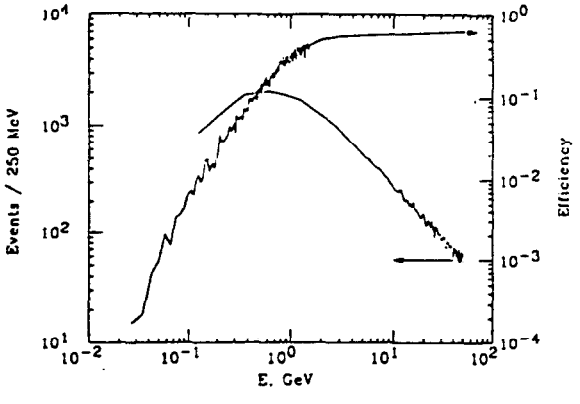

□ Figure 3. Detected photon spectrum, detection eff

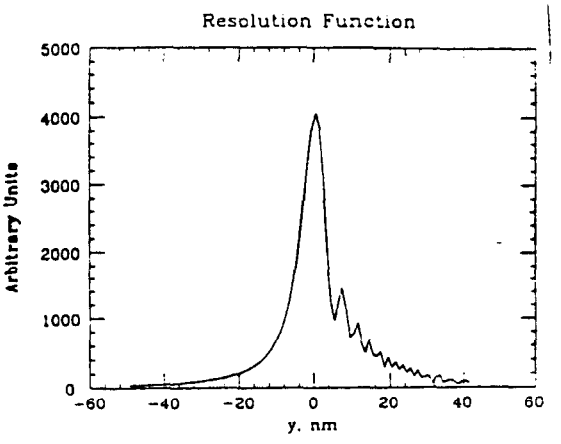

□ Figure 4. The best resolution at SLAC, $a = 2$, $b = 20$.

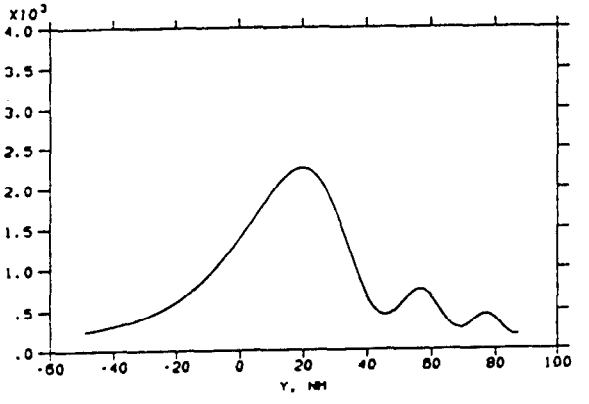

□ Figure 5. Fresnel resolution at SLAC, $a = 30$, $b = 30$.

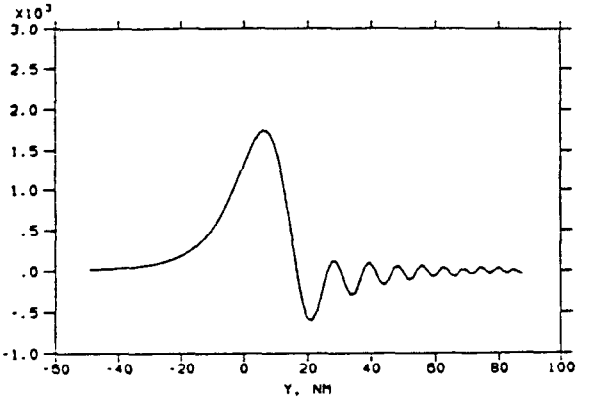

□ Figure 6. Fresnel resolution at KEK, $a = 0.5$, $b = 5$.

3.1.2 Multiple Scattering

Multiple scattering broadens the beam of electrons as they traverse the bremsstrahlung radiator. This effect can be evaluated by Monte Carlo, assuming a scattering angle of $\Theta = 13.6_{[MeV]}\sqrt{dx/L_R}/p_{e,[MeV]}$, where dx/L_R is a path length element in radiation lengths. In gen-

eral the multiple scattering correction is small as long as the beam size due to multiple scattering, s, is small compared to the unperturbed size, which essentially means that $s = \Theta t_{br} < \sqrt{\beta\epsilon}$. Results for the SLAC/FFTB and JLC/ATF final focus are shown in figure 7 and 8. These plots show the input beam profile and projections of the scattering in x and x', with the fresnel resolution.

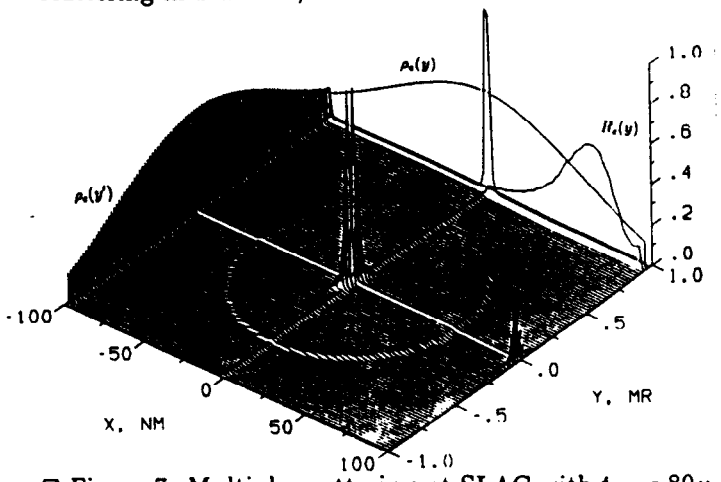

□ Figure 7. Multiple scattering at SLAC with $t_{br} = 80\mu$

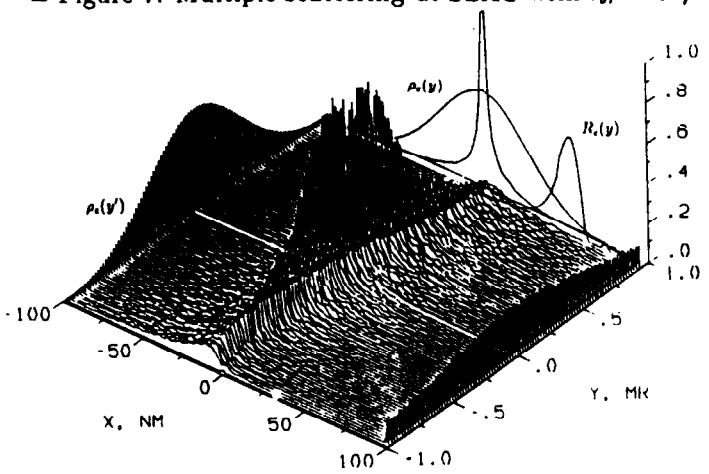

□ Figure 8. Multiple scattering at KEK with $t_{br} = 80\mu$

3.1.3 Bremsstrahlung opening angle

Bremsstrahlung photons are emitted at a small angle to the electron direction. The average angle of this emission is given by the expression $\theta_{av} = q(E_e, E_\gamma, Z)(m_e c^2/E_e) ln(E_e/m_e c^2)$, where E_e is the initial energy of the electron, Z describes the solid and E_γ is the photon energy. The function q is given by the expression $q \sim 0.80 - 0.25(E_\gamma/E_e)$, for $Z \sim 90$.[9] The bremsstrahlung opening angle has a number of secondary effects, it spreads out the image of the electron beam if viewed off axis, and it lowers brightness of the gamma beam in an energy dependent way.

3.1.4 Focusing and Synchrotron Radiation

The beam will self focus in the radiator. At SLAC, magnetic fields $B_\phi \sim \mu_0 cQ/4\sqrt{2}\pi\sigma_x\sigma_z \sim 50T$ will produce deflections, $\theta_{f,max} \sim B_\phi l/B\rho = 0.0002$. The field B_ϕ will cause synchrotron radiation, however the energy seen by the detector can be estimated from ($\theta_{f,max}$) × (loss/turn) for electrons in this field, $dE_{[GeV/turn]} = 8.8 \cdot 10^{-5} \times E^4_{e,[GeV]}/\rho_{[m]}$, which is about 0.004 J for $3 \cdot 10^{10}$ electrons. With a critical energy of $E_{c,[GeV]} = 6.6 \cdot 10^{-7} \times E^2_{e,[GeV]} B_{\phi,[T]} \sim 91$ MeV, most photons are 100 MeV or less. The total energy lost into this radiation will be much smaller than into bremsstrahlung. The spectra for synchrotron photons are compared with bremsstrahlung in figure 9, with and without efficiencies. Total energy for bremsstrahlung is ~ 24 J/pulse, so when the detection efficiency is considered the total energy in synchrotron photons is ~ 0.1% of the bremsstrahlung energy.

At KEK the comparatively low energy will produce very strong focusing forces and short focal lengths. Bremsstrahlung and Multiple scattering will also cause large photon divergences. This seems to imply that the thinnest bremsstrahlung radiators should be used at low energies.

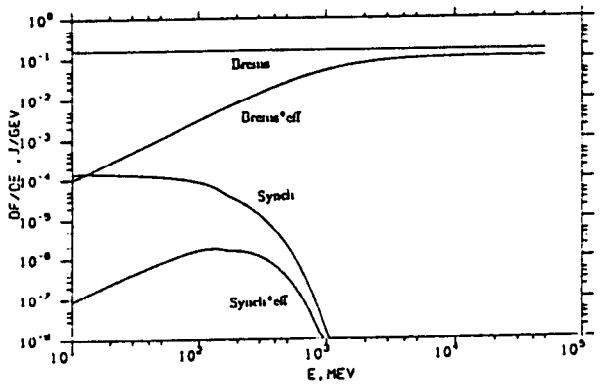

□ Figure 9. Synchrotron radiation spectra.

3.1.5 Ionization and motion of Pb atoms

The intense electron beam will ionize the bremsstrahlung radiator and these heavy ions will then be pushed toward the median plane of the electron beam which will ultimately alter the radiation length. Ionization has been calculated assuming $\sigma_{+,[Mb]} \sim 0.12Z + 0.2 \sim 10$ Mb for Pb, [5][10] with $\sigma_{++} = \sigma_+/4$, $\sigma_{+++} = \sigma_{++}/4$.[9] Figure 10 shows the result that the Pb is fully ionized, and significant double and triple ionization also occurs. Ion

motion, Fig 11, has also been calculated and this is significant. The ions are accelerated to energies of about a keV and then travel toward the median plane of the beam, where they interpenetrate to create what seems to be a very high density for a short time.

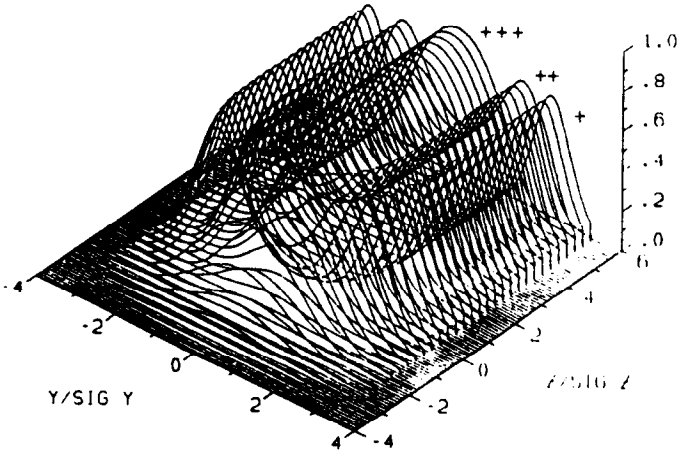

□ Figure 10. Ionization of Pb.

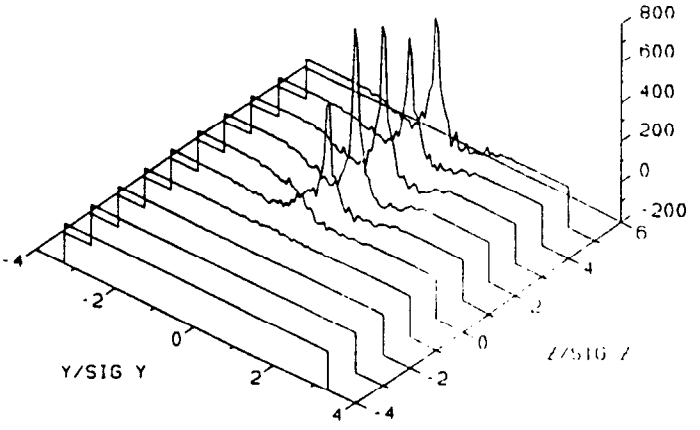

□ Figure 11. Pb ion motion.

3.1.6 Detector Acceptance

The aperture of the slits required to produce a significant signal above background will also contribute to the resolution. It is anticipated that this effect should be small relative to the Fresnel diffraction for high energy beams and multiple scattering and bremsstrahlung opening angle effects at low energies.

3.1.7 Deconvolution

The effects due to multiple scattering, bremsstrahlung and fresnel diffraction can be accurately evaluated theoretically. When combined with measurements of the slit widths, it should be possible to calculate a combined resolution function which should be able to describe the system. Precise measurements of the beam profile should be possible by then deconvolving this the observed profile with the calculated resolution function.

3.2 Backgrounds

3.2.1 Slit scattering

Slit scattering has been evaluated with EGS4. Preliminary results seem to show that the angle of secondaries is inversely proportional to their energies, and the effect can be roughly calculated by evaluating pair production and multiple scattering of the leptons. Since only the smallest angles are significant, only the first generation pairs contribute as the scattering angle approaches 0°. Figure 12 shows EGS4 results for a 50 GeV bremsstrahlung spectrum.

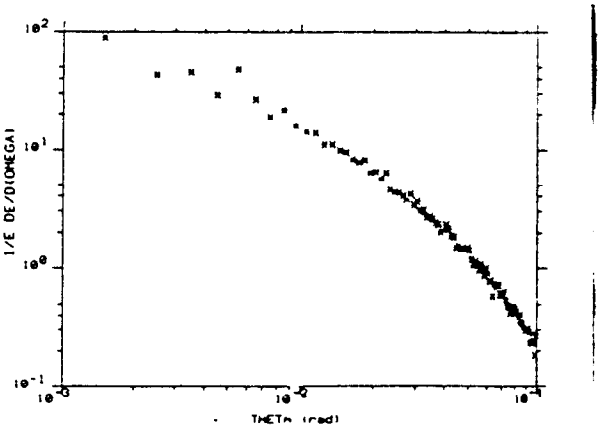

□ Figure 12. Slit scattering angles for 50 GeV bremsstrahlung.

3.2.2 Muons, Beamline showers, Synchr. rad.

To a first approximation, the system can be made blind to synchrotron radiation, which is troublesome because it is produced by the beam with very small emittance near the final focus. Although the streak camera detects visible and near UV, direct synchrotron radiation from the beam in magnets, plasmas or the primary radiator would be blocked by the bremsstrahlung radiator and pair converter. The optics of the streak camera can be made light tight.

The primary means of discriminating between signal and shower electrons is that the brightness of the signal should be much larger than that of the showers, which can be

magnetically dispersed in two dimensions. With roughly 2000 $e^{+/-}$'s produced at the pair radiator in an acceptance area, limited by slits, of $(100\mu,\ \sigma'_y * a \sim 2cm)$ times a solid angle of $(2°)^2 = 0.0012$ sr, there is an energy density of 1.7 J/r^{2}m^2 at the radiator. This compares with 80 J/bunch transmitted down the line. In addition, timing can be used to separate direct photon paths from indirect shower paths.

The environment downstream of the final focus will be inhospitable to precision equipment. Mechanical, optical and electrical components should be tested to make sure they will function in the high radiation environment.

3.2.3 Upstream Magnets

Since the energy density seen downstream from synchrotron radiation is $\sim E_e^2 B^2/\Delta z^2$, and $B_\phi \sim 1/\sigma$, where Δz is the distance between the magnetic field producing radiation and the detector, the bremsstrahlung radiator should be the dominant source of background. The self field of the focused electron beam, ($\sim$ 50 T), is higher than any other field in the line, including plasma lens fields, and the final focus is closer to the detector than another magnetic source. In addition the bremsstrahlung spot will direct synchrotron radiation toward the detector, where upstream magnets will direct their radiation away from the detector.

3.3 Transmitted electron beam

The thin bremsstrahlung target will alter the momentum and angle of the electron beam. Since the energy loss will be nonuniform, capture downstream will be more difficult. The existing EGS4 data can be used to provide an electron spectrum which can be used to increase the admittance of the downstream line with TURTLE. In the absence of benders, a FODO structure can confine a wide momentum spectrum, and it is hoped that modifications can be minimal.

3.4 Parameter Summary

The important parameters of the system are listed in the following table.

	SLAC/FFTB	JLC/ATF
E, GeV	50.	1.54
n_e	$1-3\cdot10^{10}$	10^{10}
a, m	30.	0.5
b, m	30.	5.0
t_{br}	150μ	80μ
t_{pair}, mm	3.6	3.6
t_{Ch}, cm	2.0	2.0
$\theta_{e\gamma,ms+br,[mr]}$	0.10 ($0.2\sigma_{y'}$)	1.85 ($3.7\sigma_{y'}$)
coll. material	invar	invar
rad. material	Pb, U or W	Pb, U or W
Č material	Xe	Xe
$p_{e,min}$, MeV	15.	15.
θ_γ, °	2.	2.

4 Hardware

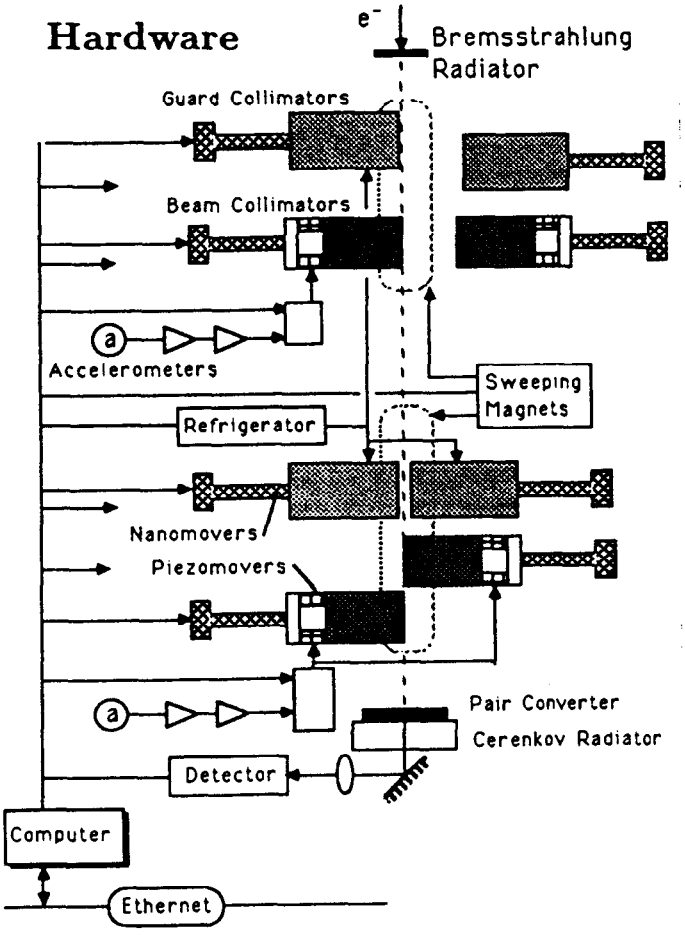

□ Figure 14. The system.

4.1 Foils

It is assumed that high Z materials will be used for the foil, and that these will be locally destroyed on every pulse. If a large foil area was inserted and loosely mounted from some point upstream or downstream of

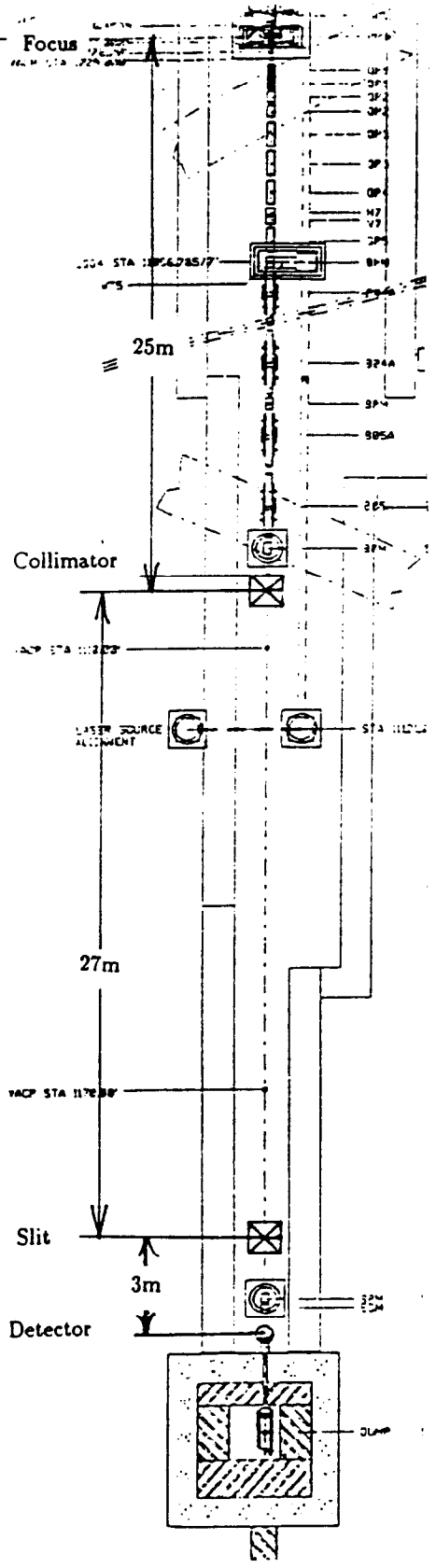

□ Figure 15. Layout

the focus, mechanical rastering the foil should be sufficient to provide a new part of the foil for every bunch, while maintaining the position along the beam line. The foil thickness should be less than β^*

4.2 Beam Collimators

Collimators can be made from commercially available metal mirrors, which are described in catalogues with a flatness of $< \lambda/40 \sim 14$ nm, and surface roughness of better than 1 nm.[11] Six invar mirrors with dimensions of $\sim$ 5 - 10 cm, optically polished to a few nm surface roughness, would cost about $3000, and take about 10 weeks to fabricate.[12] The ideal shape of the primary collimator would be slightly convex with the front edge tangent to one side of the slit and the downstream edge tangent to the other side of the slit. With a 1 μ slit opening, this would imply a sagitta of about 1 nm, which is essentially flat. It is assumed that guard collimators would be larger, heavier and perhaps water cooled, rough positioning ($\pm$ 100 nm) of these should be sufficient.

4.3 Guard Collimators

Since the primary collimators must be thermally and mechanically stable, it is difficult to simultaneously design them to absorb significant beam power. The guard collimators on the other hand should be able to absorb this power, while maintaining alignment only to the level of $\sim 0.1\mu$. Cooling must be done in a way which does not communicate vibration to the beam collimators.

It is desirable to have the collimators operate in a magnetic field to disperse the showers in as large a solid angle as possible. While high field would be desirable, the aperture of these magnets need not be much larger than the dimensions of the collimators they work with, (5 - 10 cm).

4.4 Detector

To examine the penumbra with high resolution, it is necessary to use a slit just before the convertor. A precollimator is inserted upstream of the open side of the slit to reduce shower backgrounds on it. It is assumed that Xe gas at 1 atm can be used as the Čerenkov radiator. With a refractive index $n = 1.00071$, the opening angle of radiation is 2.1°, and the minimum detectable electron energy is $\sim$ 12 MeV. This paper assumes that the pair converter is U 3.6 mm thick and the Č radiator is 2 cm thick, and the combined width due to pair production / shower dimensions and Čerenkov optics is $\sim 100\mu$. In this

geometry, electrons are efficiently used, as the Čerenkov source is inherently slitlike, and the slit on the streak camera may be unnecessary.

Time resolution within the bunch, using a streak camera, adds the requirement that the maximum amount of light be available for high resolution streak pictures. In the Argonne AATF, streak camera measurements have been done with $3 \cdot 10^{10}$ electrons imaged roughly 1X on a slit set at about 100 μ, using 2 mm of Xe at atmospheric pressure, giving long, bright streaks.[13][14] For simple intensity measurements, shorter streaks should be sufficient, which should require $I_e \sim 8 \cdot 10^7$ [$e^- mm_{Xe}$], with $I_e = n_e(l/L_R)\eta(\phi/\sigma_{x',\gamma})\Delta z$, where n_e is the number of electrons, l/L_R is the thickness of the bremsstrahlung radiator in radiation lengths ,L_R, η is the number of electrons detected for one equivalent full energy photon on the detector, which is calculated by monte carlo and is roughly 1 - 10 depending on detector, $\phi/\sigma_{x',\gamma}$ is the acceptance of the detector divided by the divergence of the photon beam, and Δz is the length of Čerenkov radiator. The bremsstrahlung radiator should have a small radiation length and its thickness should be $\sim \beta$.

For high spatial resolution, the number of detectable photons would be $n_\gamma \sim (150_{[1/cm]} n_e L_{[cm]} \sin^2\theta_C$,[15] which would yield $\sim$ 2000 photons in one Fresnel half width. This photon flux could be detected by a number of devices such as photomultiplier hodoscopes and microchannel plate / CCD camera systems.

4.5 Alignment

Rough alignment can be done with standard techniques using transit and levels. Alignment of the collimator surfaces directly parallel to the beam can be done with optical lenses and prisms, which have angular tolerances of $\pm$ 30 arc seconds, or 0.14 mrad. More precise alignment of the collimators would probably require the beam on target. Preliminary measurements could be done with the final slit opened very wide, to get a large signal.

4.6 Movers

Rough positioning of collimators can be done with a number of commercially available systems, such the the Nanomover sold by Melles Griot, which can set 20 kg loads with $\pm$100 nm resolution over 25 mm.[11] The primary collimator and final slit would have to be more carefully positioned, possibly to tolerances of $\pm$1 nm. Fine adjustment can be done with piezoactuators or Inchworm drives, sold by Burleigh, for motions of 0.1 nm to 10 μ or larger.[16] It is assumed that the collimators will each be controlled with three actuators, and the precision adjustment of these would be done in real time. Mirrors can be mounted to the structure in a number of ways, a compliant mount, such as pitch, might be desirable.

4.7 Seismic Stabilization

Since ground vibrations occur at the level of about $\sigma_v \sim 0.035\mu, \sigma_h \sim 0.1\mu$, the beam defining collimators must at least be stabilized against the vertical motion.[17] This can be done with commercial accelerometers and piezoactuators as shown in Figure 14, although the ultimate precision depends on the frequency, since the acceleration is a function of the frequency and amplitude $a = \omega^2\sigma_{x,y}$ and the ultimate resolution of commercial accelerometers is in the range of 0.3 μg. It seems possible to use such techniques as adding a number of accelerometers in parallel, digital filtering and feed forward to increase sensitivity of the system. The cost of some accelerometers is small enough ($\sim$ 500$) to make paralleling them a cost effective way to produce a sensitivity increase of $n_a^{1/2}$, as more sensitive single units are considerably more expensive. There are a number of options which can be explored with vendors, and cooperative development will be explored with any companies interested in developing all part of the system.

4.8 Shielding and Cooling

Additional shielding is required for three purposes: 1) minimizing backgrounds in the detectors, 2) minimizing heating on the collimators and support frames, and 3) minimizing radiation levels outside the shielding. In principle these are problems which can be solved using standard procedures.

Since the FFTB is being shielded for $\sim$ 2.5 kW of beam power and the bremsstrahlung radiator is anticipated to be 0.1 radiation lengths thick, it is likely that the shielding and cooling of the collimator assemblies must be able to deal with about 250 W of beam power. Since thermal expansion of components will significantly affect the alignment, critical components must be designed either to absorb power or to avoid the beam spray. It is anticipated that local shielding can protect the majority of the apparatus from the scattered beam however some moveable guard collimators will likely absorb significant heat. Since vibration motion is critical, it is necessary to be able to cool these components by some means which avoids water turbulence. The simplest solution might be an ice water bath, or some other compound which absorbs considerable heat in changing phase. On the other hand low

velocity water cooling channels may also be an acceptable solution.

4.9 Transmitted Beam Control

It is anticipated that additional quads downstream of the IP should solve the most serious problems associated with this effect. The problem can be pursued in detail when beam TURTLE is running with physical beam line elements.

4.10 Control System

The overall system can be controlled fairly easily with a small computer which can run the apparatus as well as transmit beam profile information to the main control area. It is anticipated that commercial software and hardware would be used in the monitoring system to minimize development time and permit maximum flexibility. Little specialized control equipment should be required other than the stabilization system. It is not clear at this time if online digital processing will we useful in seismic stabilization.

5 Required Development

In order to produce the best possible resolution it is necessary to use or slightly extend the state of the art in mechanical stabilization of seismic vibration with the most sensitive detectors, while actively cooling components. In addition the particle detector of the system must be designed, constructed and tested.

5.1 Seismic stabilization

If no commercial products are available, it may be necessary to build an active seismic stabilization system, as shown in Fig 14. In principle the design of this is straightforward, however operating in the limit of low frequencies and high precision will be difficult, and may require systems for enhancing signal/noise output of accelerometers. Commercial suggestions will be requested.

5.2 Image generation

It seems likely that commercially available multichannel plate detectors will be the best way to generate an image. It may also be possible to gate them with with comparatively tight timing to avoid the background due to showers near the beam dump. Other systems may have advantages, however. In addition to hardware problems, software will have to be developed which can process and display the images which are generated.

6 Cost and Schedule

Equipment costs can be estimated roughly from catalogue prices and other sources, and are included below. These costs are estimates, as a complete self-consistent design has not been produced. Personnel costs are not included in this tabulation.

Total			124
	Movers		31
		controller	10
		8 units	8
		Accelerometers	10
		long cables	3
	Optics		27
		MCP/CCD	12
		optical slits	3
		table	2
		e^+e^-, $\check{C}$ conv	10
	Mechanical		36
		collimators	4
		cooling	17
		mounts	10
		br. foil cont.	5
	Misc Controls		30
		Computers, software	20
		Thermocouples	2
		Refrigerator	5
		Temp Control	3

It is unclear at this time if the cost of piers, sweeping magnets, beam control, vacuum pipe, pumps and specialized shielding should be included in this proposal since some of this will be part of the beam dump. Their cost is also unclear.

6.1 Beamline Construction Schedule

The assembled system must be operational when the beam comes on in Jan 1993. Other time constraints will be set by the date at which construction of piers and other hardware in the tunnel must be completed by out-

side vendors.

6.2 Monitor Development Milestones

• Sept 30, 1991: Complete Design Document

Will contain local shielding requirements obtained in consultation with SLAC, component positions, pier requirements, and design of: collimators, movers, cooling, alignment procedure, any sweeping magnets, detectors, control system, software and suggested interfaces with existing control systems.

• Mar 30, 1992: Demonstration of Seismic Stabilization and Image Generation

Should be a demonstration at Argonne of two crucial elements of the system

• Sept 30, 1992: Delivery of all systems at SLAC

Will include delivery and installation of all hardware and software, along with design drawings and some written description of the control procedures.

7 People

Since the tasks associated with the development of this system are not those traditionally associated with HEP, there are useful benefits involved in doing them in a multipurpose lab where there are people experienced and equipped for seismic measurements and a wide variety of nuclear instrumentation. At the same time it seems possible to use the ANL HEP Instrumentation Group to help design and construct any specialized electronics and the overall control system.

8 Acknowledgements

P. Schoessow of ANL produced EGS4 calculations of showers in slits, and G. Fischer of SLAC has provided information on vibration and surveying techniques.

References

[1] R. B. Palmer, Annu. Rev. Nucl. Part. Sci. 40, 529, ('90)

[2] J. Norem, Proceedings of the 1988 Linear Accelerator Conf., Newport News, Virginia, (1988), p430

[3] K. Oide, Proc. 1989 Particle Accelerator Conf, Chicago, 1989, p1319

[4] K. Oide, KEK, private communication, (1991)

[5] J. Buon, F Couchot, J. Jeanjean, F. LeDiberder, V Lepeltier, H. Nguyen Ngoc, J. Perez-y-Jorba, M. Puzo, and P. Chen, Nucl. Instr. and Meth., accepted for publication, (1991)

[6] T. Shintake, Proposal of Nano-meter Beam Size Monitor for e^+e^- Linear Colliders, KEK Preprint 90-173, KEK, (1990)

[7] Jenkins and White, Fundamentals of Optics, Fresnel Diffraction, McGraw-Hill (1957)

[8] H. A. Bethe, in Experimental Nuclear Physics Vol 1, E. Segre, ed., John Wiley and Sons Inc. New York, (1953), p166

[9] B. Rossi, High Energy Particles, Prentice-Hall Inc, Englewood Cliffs N. J., (1952)

[10] P. Chen, Contribution to NLT Workshop SLAC, (1988)

[11] Melles Griot, Irvine Calif. 92714

[12] R Lowrey, Rockwell Power Systems, Albuquerque NM (private communication)

[13] J. B. Rosenzweig, P. Schoessow, B. Cole, C. Ho, W. Gai, R. Konecny, S. Mtingwa, J. Norem, M. Rosing, and J. Simpson, Phys. Fluids B 2, 1376, (1990)

[14] Hamamatsu Photonic Systems Corp., Bridgewater, NJ, 08807

[15] J. Litt and R. Muenier, Annu. Rev. Nucl. Part. Sci., 23, 1, ('73)

[16] Burleigh Instruments Inc., Fishers, NY, 14453

[17] R. E. Ruland, G. E. Fischer, Proceedings of the 2nd International Workshop on Accelerator Alignment, Hamburg, Germany, Sept 10-12, 1990. and Stanford Linear Accelerator Laboratory publication SLAC-PUB-5326 (1990)